

UNIVERSIDAD SAN FRANCISCO DE QUITO USFQ

Colegio de Ciencias e Ingenierías

**Influence of an Electromagnetic Field in the Adhesion
Strength of Ni-based Alloys in Thermal Spray**

Trabajo de Investigación

Andrés Patricio Sánchez Ruiz

Ingeniería Mecánica

Trabajo de titulación presentado como requisito
para la obtención del título de
Ingeniero Mecánico

Quito, 18 de mayo de 2018

UNIVERSIDAD SAN FRANCISCO DE QUITO USFQ
COLEGIO DE CIENCIAS E INGENIERÍA

**HOJA DE CALIFICACIÓN
DE TRABAJO DE TITULACIÓN**

**Influence of an Electromagnetic Field in the Adhesion Strength of Ni-based
alloys in Thermal Spray**

Andrés Patricio Sánchez Ruiz

Calificación:

Nombre del profesor, Título académico

Alfredo Valarezo, Ph.D.

Firma del profesor

Quito, 18 de mayo de 2018

Derechos de Autor

Por medio del presente documento certifico que he leído todas las Políticas y Manuales de la Universidad San Francisco de Quito USFQ, incluyendo la Política de Propiedad Intelectual USFQ, y estoy de acuerdo con su contenido, por lo que los derechos de propiedad intelectual del presente trabajo quedan sujetos a lo dispuesto en esas Políticas.

Asimismo, autorizo a la USFQ para que realice la digitalización y publicación de este trabajo en el repositorio virtual, de conformidad a lo dispuesto en el Art. 144 de la Ley Orgánica de Educación Superior.

Firma del estudiante:

Nombres y apellidos:

Andrés Patricio Sánchez Ruiz

Código:

00117122

Cédula de Identidad:

1719734939

Lugar y fecha:

Quito, 18 mayo de 2018

ACKNOWLEDGMENTS

Nobody has been more important to me in the pursuit of this project than my parents, whose love and guidance are with me in whatever I pursue. Also, I truly thank to my loving girlfriend Gabriela, who provided motivation and continuous support. Last but not the least, I would like to express my sincere gratitude to my friend and advisor Alfredo Valarezo for sharing his vast knowledge.

RESUMEN

Las modificaciones de las propiedades de un recubrimiento dadas por un adecuado control del proceso pueden sustancialmente mejorar el desempeño del recubrimiento. En este estudio, es de interés desarrollar un nuevo parámetro de control, en este caso, campo electromagnético externo para influenciar la fuerza de adhesión. En este estudio, el efecto de un campo electromagnético aplicado en dirección perpendicular (0.15 – 0.35 [T]) y paralela (0.04 – 0.09 [T]) a la superficie del sustrato durante el proceso de termorociado ha sido investigado. Se observó que el campo electromagnético afecta dramáticamente la formación de *splats* (partículas impactadas) de aleaciones con base de níquel y, por ende, la formación de la interface intersplat/sustrato. La fuerza de adhesión/cohesión de los recubrimientos por termorociado fue puesta a prueba cumpliendo el estándar ASTM C633-13, donde se encontró una disminución en la adhesión de un 30% para las muestras influenciadas con campo electromagnético sin importar la dirección. Además, la variación en la morfología del splat fue estudiada por microscopía electrónica de barrido, y se encontró una tendencia a formar splats con forma de disco y una reducción del salpicado de splats cuando se aplica el campo electromagnético. Se discute las potenciales causas de esta influencia. Esta investigación abre un nuevo campo de estudio que puede permitir la introducción de diseños de campos electromagnéticos que causen un efecto positivo a la rápida solidificación y, por ende, a la microestructura de recubrimientos por termorociado.

Palabras clave: Campo electromagnético; Aleaciones de Níquel; Adhesión; Morfología del splat; Formación de Splat, Adhesión, Termorociado.

ABSTRACT

Modification of coating properties by adequate process control can substantially improve coating performance. In this study, it is of interest to develop a new process control parameter, that is, external electromagnetic field, to influence adhesion strength. In this regard, the effect of a high electromagnetic field applied in a direction perpendicular (0.15 – 0.35 [T]) and parallel (0.04 – 0.09 [T]) to the substrate surface during thermal spray process was investigated. It was observed that the electromagnetic field affects dramatically the splat formation of Ni-based alloys, and thus the intersplat/substrate interface formation. Adhesion/Cohesion strength of the thermal spray coatings was tested under the ASTM C633-13 standard, and it was observed that adhesion has been weakened by 30% for samples with electromagnetic field influence no matter the direction. Furthermore, the variation in splat morphology was studied by scanning electron microscopy: a tendency of forming disk-shaped splats and a reduction of splat splashing were found while applying the electromagnetic field. The potential causes of this influence are discussed. This investigation opens a new field of study that may allow the introduction of design-based modifications to the electromagnetic fields to cause a positive effect on the rapid solidification and thus, to the microstructure of thermal spraying coatings.

Keywords: Electromagnetic field, Ni-based alloys, Splat morphology, Splat Formation, Adhesion, Thermal spray.

CONTENTS

Resumen	5
Abstract	6
Contents.....	7
List of Tables.....	8
List of Figures	9
Introduction	10
Experimental Methods	17
Materials	17
Methodology	21
Characterization	23
Results and Discussion.....	24
Conclusions	35
References	37
Appendix A: Detailed Drawings	38
Substrate.....	38
Electromagnet #1: Receptacle – Core.....	39
Electromagnet #1: Assembly	40
Electromagnet #2: Core	41
Electromagnet #2: Receptacle.....	42
Electromagnet #2: Assembly	43
Self-Aligning Device: Parts	45
Self-Aligning Device: Assembly	46
Counterpart Holder	47

LIST OF TABLES

Table 1. Number of samples produced by flame spaying.....	22
Table 2. Spraying parameters for sample preparation.....	22

LIST OF FIGURES

Figure 1. Schematic drawing of the splat formation process.....	13
Figure 2. Splat formation process influenced by a d.c. electromagnetic field perpendicular to the substrate surface.....	14
Figure 3. NiCrBSiFe splats by flame spray.....	15
Figure 4. Splat formation process influenced by a d.c. electromagnetic field parallel to the substrate surface.....	15
Figure 5. Electromagnet #1: Magnitude and direction of electromagnetic field simulated with FEMM.....	18
Figure 6. Electromagnet #1: Magnitude and direction of electromagnetic field simulated with FEMM.....	19
Figure 7. Schematic drawing of the experiment set-up.....	20
Figure 8. Experiment set-up, front view.....	20
Figure 9. Experiment set-up, top view.....	21
Figure 10. SEM images of powders used for thermal spraying.....	24
Figure 11. First trial, typical Ni splats by flame spray.....	25
Figure 12. First trial, typical Ni splats by flame spray, using SEM.....	26
Figure 13. Second trial, typical Ni splats by flame spray.....	28
Figure 14. Typical NiCr splats by flame spray.....	29
Figure 15. Typical NiCrBSiFe splats by flame spray.....	31
Figure 16. NiCrBSiFe with parallel electromagnetic field influence.....	32
Figure 17. Ni coating by flame spray.....	32
Figure 18. Adhesion strength of coatings with and without electromagnetic influence during deposition.....	33

INTRODUCTION

Thermal Spray (TS) technology is a coating process that has been continuously developed over the past five decades. The goal of this technology is to produce coatings for wear resistance, corrosion barriers, and thermal protection; as well as to improve electric, friction, and magnetic properties (Fauchais, Vardelle, & Dussoubs, 2001). This coating process has been used worldwide because of its tremendous benefits, achieved owing to not only the academy but the industry, that have invested billions of dollars in R&D. The global thermal spray market revenue was approximately USD 8.1 billion in 2016 and it is expected to reach USD 12.62 billion in 2022 (Mordor Intelligence, 2016). TS is being used by industrial markets such as aerospace, automotive, petroleum, electric generation, electronics, and biomedicine. It is noteworthy that the aerospace and automotive industries have the most influence in this market. The applications for the aerospace industry include enhancing and protecting the expensive landing gears and aircraft engine components. For the automotive industry, the key objective is to extend the service life of coated automotive parts such as pistons and crankshafts. To lead the global coating market, the quality assurance and the continuous improvement of coating reliability is a priority.

There is an important interest around the process control toward producing desired property values that any coating processing system performs. Researchers deeply study and understand the causes of this property variability, while engineers apply the improved process to produce higher quality coatings. In TS, the most important coating properties that affect directly the engineering usage of this process are: adhesion between the coating and the substrate, and cohesion between each coating layer (Fauchais, Fukumoto, Vardelle, & Vardelle, 2004). Thus, any R&D efforts towards improving these properties are worth.

In TS molten particles are sprayed at high temperatures and high velocities onto a surface. Individual molten particles, called droplets, impact on the substrate forming “splats”

that pile up one on top of the other creating the deposit or coating layers (Sampath & Jiang, 2001). Thus, there is an intrinsic relationship among the adhesion and cohesion property (and others, like chemical, thermoelectric, and mechanical properties) with the quality of contact between splats and the substrate or previously deposited coating layers, respectively. If the coating does not adhere properly to the substrate, it will never protect it (Chandra & Fauchais, 2009).

The quality of contact between splats and the substrate is correlated with splat formation. To increase adhesion and cohesion, i.e. increase the quality of contact, there should be an improvement of the splat quality. That is why the splat formation process is a major concern during the thermal spray process, and there are several studies related to the effect of various parameters on this process. For instance: with an increase of substrate temperature to 200 – 400 °C the splat morphology changes from fragmented to a contiguous disk-shaped with limited or no splashing (Sampath & Jiang, 2001); and on rough surfaces (roughness > 0.2 [μm]) there is a poorer splat-substrate contact than on smooth surface (roughness < 0.2 [μm]), and this could lead to the formation of fingered-shaped splats if the rough substrate was not preheated. Not only the substrate temperature and the surface roughness affect the substrate but also the ambient pressure, presence of adsorbates and condensates, hardness of the substrate, spray angle, and the particle state are variables that can be controlled to enhance the splat formation.

Modifying and varying some parameters during thermal spraying can substantially improve coating properties. However, there is not an extensive study of magnetic field influence in splat formation. Until now, there is only two previous investigations, the first one conducted at the King Mongkutt's University of Technology Thonburi, where the effects of a magnetic field in poly(ether-ether-ketone) coatings in TS has been studied (Tharajak, Palathai, & Sombatsompop, 2017). It has been found that the magnetic field improves the

coating properties of PEEK, reducing the friction coefficient and increasing the wear resistance of the sprayed coating. The second previous research was conducted at Universidad San Francisco de Quito, where the effects of an electromagnetic field during solidification of Ni-based alloyed splats has been studied (Recalde, Castro, Bejarano, Vargas, & Valarezo, 2017). It has been found that the electromagnetic field reduces the spreading and determines deep craters on the top of the splats, and also that the adhesion strength was increased by 25% for NiCrBSiFe coatings by flame spray.

Electromagnetic fields in the processing of materials are used to enhance properties in many different processes, including casting of metals, and growth of semiconductors. In the solidification processes for molten metals, an alternating current (a.c.) electromagnetic field is used to generate strong flow motion of the molten metal specially during pouring of castings, meanwhile, a direct current (d.c.) electromagnetic field is used to reduce unwanted turbulent flows during solidification (Li, 1998). The Lorentz force \mathbf{f} , caused by the interaction between a magnetic field \mathbf{B} and a current density \mathbf{J} , is the force that interacts with the fluid in motion during the flow of molten material (Asai, 2006). F can be expressed as

$$\mathbf{F} = \mathbf{J} \otimes \mathbf{B} \quad (1)$$

A conductive fluid motion in a magnetic field induces an electric current, indeed Ohm's law is extended to

$$\mathbf{J} = \sigma(\mathbf{E} + \mathbf{v} \otimes \mathbf{B}) \quad (2)$$

where σ is the electric conductivity, \mathbf{E} is the electric field induced by change of a magnetic field with time, and \mathbf{v} is the local fluid velocity, then Eq. 1 can be written as

$$\mathbf{F} = \sigma(\mathbf{E} + \mathbf{v} \otimes \mathbf{B}) \otimes \mathbf{B} \quad (3)$$

With the usage of d.c. electromagnetic fields since there is not an induced electric field E in the fluid, so the Lorentz force becomes

$$\mathbf{F} = \sigma(\mathbf{v} \otimes \mathbf{B}) \otimes \mathbf{B} \quad (4)$$

Micro-scaling these concepts to splats formation under the effects of electromagnetic fields, the possible modifications to splat formation can be remarkable. The splat formation process can be divided into three general steps as illustrated in Fig. 1. First, the TS powder is heated and accelerated by the flame spray; then the molten or partially molten particle with in-flight velocity (bellow 100 [m/s]) impacts onto the substrate; and finally the particle suffers flattening and spreading on the substrate surface driven by dynamic impact and inertia of the particle (Yang, Liu, Zhou, & Deng, 2013). This impact phenomena lasts a few microseconds for splat flattening and 3 – 10 microseconds for splat solidification to be completed, indeed a splat is entirely formed in 10 - 20 microseconds (Fauchais et al., 2004).

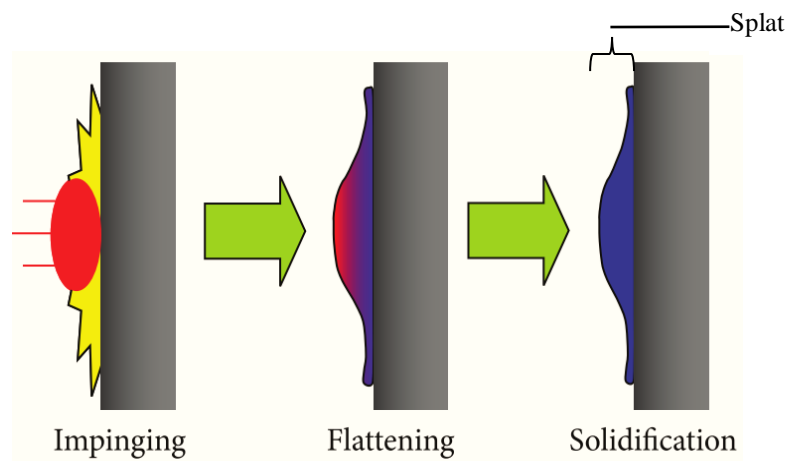


Figure 1. Schematic drawing of the splat formation process. Adapted from “Recent Developments in the Research of Splat Formation Process in Thermal Spraying,” by Yang et al., 2013, Journal of Materials, Volume 2013, Copyright © by Kun Yang et al.

Right after the particle/substrate collision, the molten particle starts to flow laterally with local velocities (on the lower range compared to the in-flight velocity) parallel to the surface. The rapid solidification occurs typically after the spreading has occurred. This rapid

solidification process can be influenced by an electromagnetic field of hundreds of mT, therefore it is hypothesized that applying a d.c. electromagnetic field directed perpendicular (or parallel) to the substrate surface while the splat formation process occurs, substantial changes on splat morphology will be observed. As it is shown in Fig. 2, Lorentz forces opposes the local fluid velocity when a perpendicular electromagnetic field is applied; this influence could act as a fluid flow suppression, hence splashing could be reduced and more likely disk-shaped splats could be obtained, as observed by Recalde et al. (Recalde et al., 2017). The suppression effect occurs while the splat is in the liquid state. Indeed, the final splat diameter should be reduced considerably.

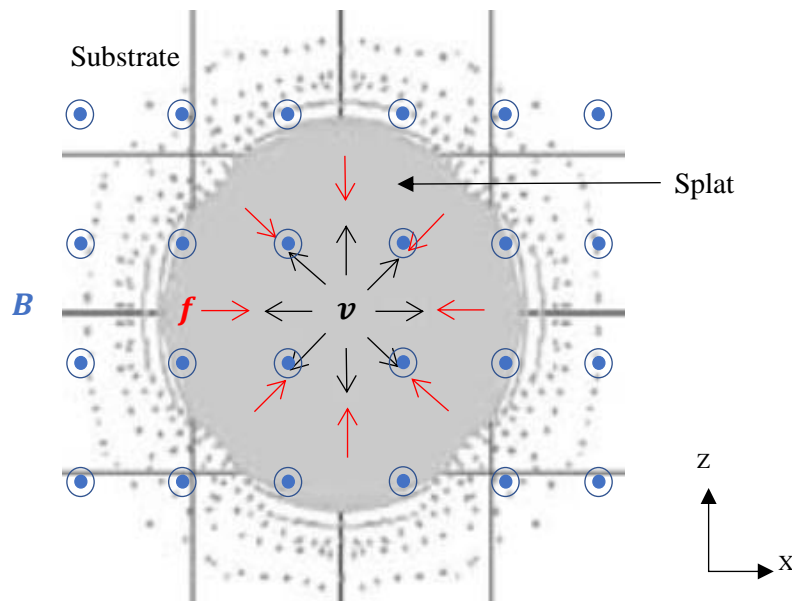


Figure 2. Splat formation process influenced by a d.c. electromagnetic field perpendicular to the substrate surface. B : electromagnetic field pointing outward; v : fluid velocity; f : Lorentz force.

This theory has a complete correlation with the results obtained by Recalde, O. As illustrated in Fig. 3b, the splat obtained under the influence of an electromagnetic field has an identifiable dimple in the center. Profilometry images of Recalde's research showed that the electromagnetic field reduced significantly the spreading and concentrated mass near the center, thus the fluid flow suppression theory could be the reason of this phenomenon.

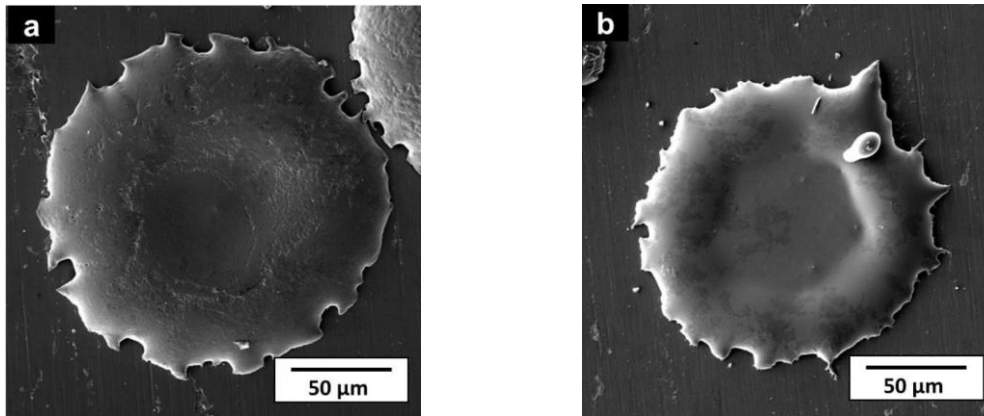


Figure 3. NiCrBSiFe splats by flame spray: typical splat deposited a) without applied electromagnetic field; and b) with electromagnetic field. Adapted from “Recalde, O., Castro, W., Bejarano, M. L., Vargas, M., & Valarezo, A. (2017). Effect of Electromagnetic Field during Solidification of Ni-Based Alloyed Splats. In International Thermal Spray Conference & Exposition (ITSC 2017) (pp. 577–581). Dusseldorf: Curran Associates, Inc.

When a parallel electromagnetic field is applied, the Lorentz Force could only suppress the z -component of each local velocity \mathbf{v} since the x -component will result in $\mathbf{F} = 0$, as illustrated in Fig. 4. This type of influence could be seen as a controlling shape process where the splat experiments flow suppression in z -direction while free motion in x -direction.

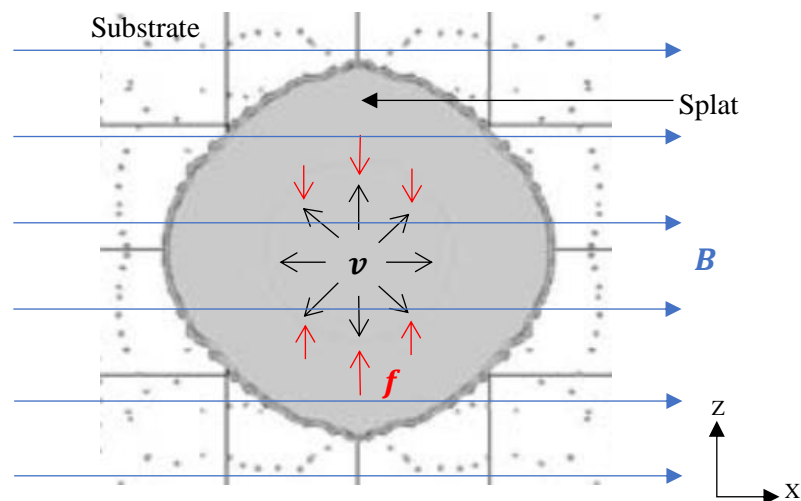


Figure 4. Splat formation process influenced by a d.c. electromagnetic field parallel to the substrate surface. \mathbf{B} : electromagnetic field; \mathbf{v} : fluid velocity; \mathbf{f} : Lorentz force.

For both cases, perpendicular and parallel, the Hartmann number should be determined. The Hartman number is the ratio of electromagnetic forces to the viscose forces,

if this number is below 1 the viscous forces dominate and if it is above 1 the electromagnetic forces dominate (Schlangen, 2013). The Hartmann number Ha is calculated as:

$$Ha = BL\sqrt{\frac{\sigma}{\mu}} \quad (5)$$

where B is the magnetic field, L is the characteristic length, σ is the electrical conductivity, and μ is the dynamic viscosity.

Considering the above mentioned possible effects of magnetic field in the flow of droplets, the aim of this study is to determine the influence of an electromagnetic D.C. field, parallel and perpendicular to the substrate surface, on splat morphology and formation during processing, and to observe the effect on adhesion and cohesion of the coating, particularly in flame spraying with Ni-based powders. Adhesion/cohesion testing was carried out based-on ASTM C633-13 Standard Test Method for Adhesion or Cohesion Strength of Thermal Spray Coatings. Finally, the study discusses the possible explanations of this influence.

Establishing the understanding of such influence of the electromagnetic fields in splat formation could change the practice of the coating technology providing a new tool to improve coating properties (in this case, adhesion/cohesion), towards satisfying the necessities and the strict requirements of the market. Additionally, it could reduce the gap between the industry and the academy providing an innovative control parameter. Also, it could be the gate for future studies to fully understand this influence. Factors such as particle coalescence, splat splashing, and splat morphology could be modified, and potentially improve and engineer coating-surface interfaces and inter-splat interfaces (Recalde et al., 2017).

EXPERIMENTAL METHODS

Materials

Ni (Metco 56C-NS, NY, USA), NiCr (Metco 43F-NS, NY, USA) and NiCrBSiFe (Eutalloy 11496, Castolin Eutectic, WI, USA) powders were thermally sprayed by the flame spray technique onto steel substrates to obtain splats and coatings. A flame spray torch (Metco 5P-II, NY, USA) was used for thermal spraying. The substrates were cylinders with a diameter of 25.4 [mm] (1 [in.]), length of 38.1 [mm] (1.5 [in.]) and were made out of AISI 1018 low carbon steel. A detailed drawing is shown in appendix A. This material was selected because of its ferromagnetic property, it has a relative magnetic permeability of 840, making it a suitable material for electromagnet cores. Also, AISI 1018 steel is commonly used as a substrate material in thermal spray applications. The substrate surfaces used for splat collection were polished with a 240-grit sandpaper until a 1 [μm] suspension solution of alumina particles, whereas the substrate surface used for coatings were sandblasted with aluminum oxide 46-grit and 90 [psi] of compressed air.

Two electromagnets were designed and fabricated to produce the required magnetic field. To design the electromagnets, simulations were performed using the Finite Element Method with Magnetics software (Version 4.2; Meeker, 2015). The first electromagnet, called here as Electromagnet #1, has a solenoid configuration imposing a field perpendicular to the substrate surface. Since the Electromagnet #1 is symmetric, the axisymmetric environment of FEMM can be used. Several trials were performed varying the length of the core, the diameter of the core, the number of coil turns, and the applied current. For the interest of this investigation, the magnitude of the field produced at substrate's surface was of vital importance. It was found that the magnetic field is directly proportional to the number of turns and the current. Also, if the length of the cylindrical core increases, the magnetic field

at the substrate surface decreases. And finally, the magnetic field increase with the core radius, i.e. the magnetic field is bigger at the external radius than at the center of the core.

At the end of the simulation, the parameters that best fit the requirements has its core made of AISI 1018 low carbon steel and has a receptacle where the substrate sample can be placed. The coil was made of isolated copper wire AWG 15 and has 750 turns. A power supply of 7 amperes was established in the simulation resulting in a magnetic field that varies from 110 to 350 mT at the surface, as illustrated in Fig. 5. The highest magnitude is located at the external radius of the substrate whereas the lowest is at the center of the substrate.

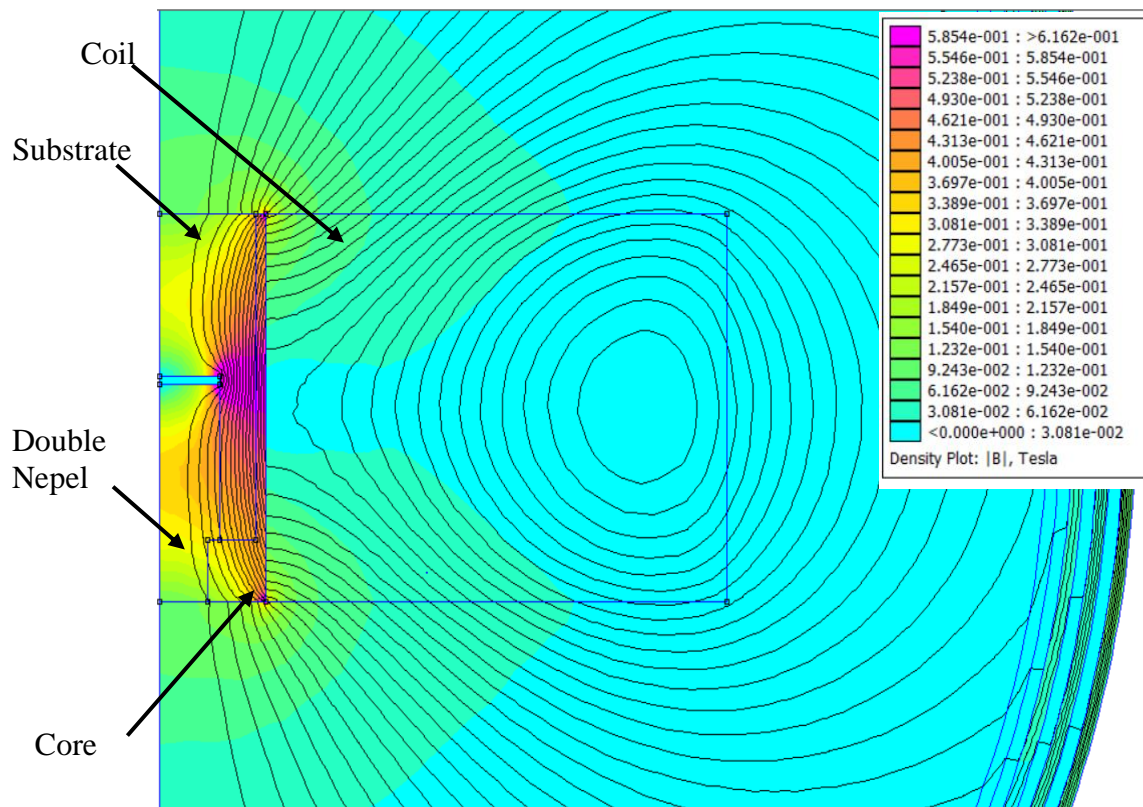


Figure 5. Electromagnet #1: Magnitude and direction of electromagnetic field simulated with FEMM.

The second electromagnet, Electromagnet #2, has a C-core configuration imposing a field parallel to the substrate surface; this configuration was used because a parallel magnetic field can be produced between the two C branches. The electromagnetic field generated by this electromagnet was simulation with FEMM. It was found that if the air gap between the branches is smaller, the magnetic field can be increased. At the end of the simulation, the

parameters that best fit the requirements has its core made of silicon electrical steel and had a polymer receptacle (non-magnetic material) between the C branches where the substrate sample can be placed. The coil was made of isolated copper wire AWG 20 and had 800 turns. A power supply of 4 amperes was established in the simulation resulting in a magnetic field parallel to the substrate surface that varies from 90 to 130 mT, as illustrated in Fig. 6. In contrast of Electromagnet #1, the electromagnetic field tends to be constant in all the substrate's surface.

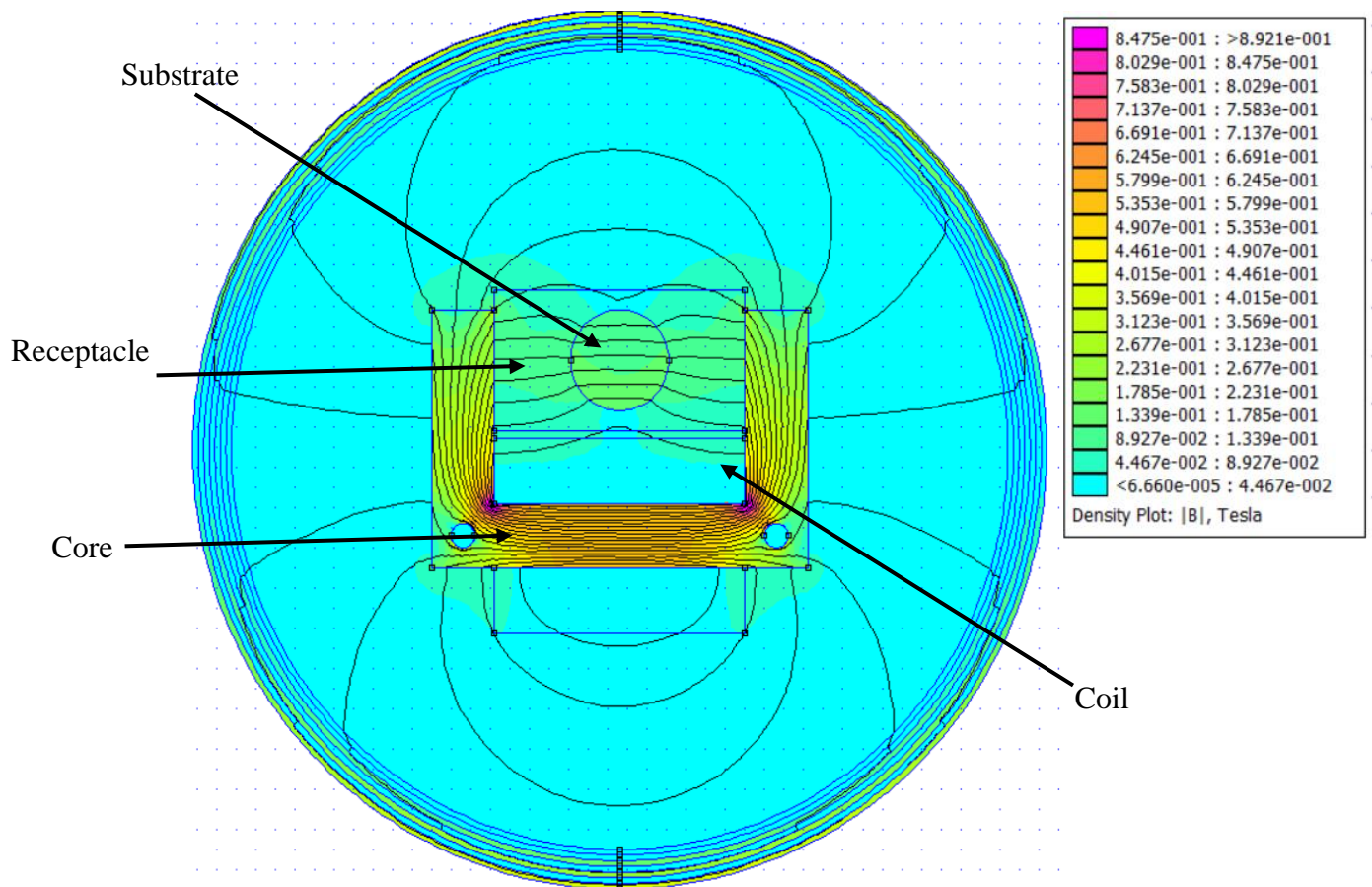


Figure 6. Electromagnet #2: Magnitude and direction of electromagnetic field simulated with FEMM.

A DC power supply (Agilent Technologies E3633A, CA, USA) of 7 amperes and 24 volts was used to power the electromagnets. The current used for electromagnet #1 and #2 were 7 [A] and 4 [A] respectively, and both electromagnets were covered with glass wool to

protect them from the high temperatures produced by the thermal spray gun. A schematic drawing and an actual photo of the experiment set-up is shown in the figures 7-9.

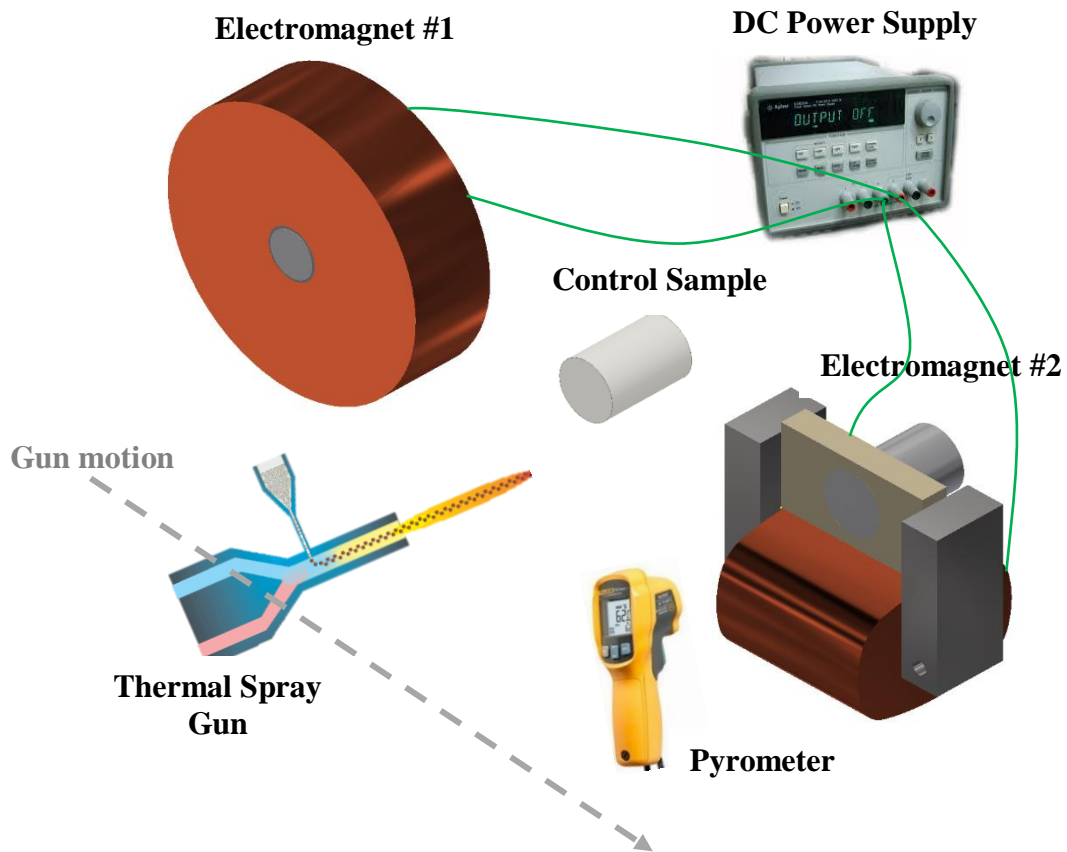


Figure 7. Schematic drawing of the experiment set-up.

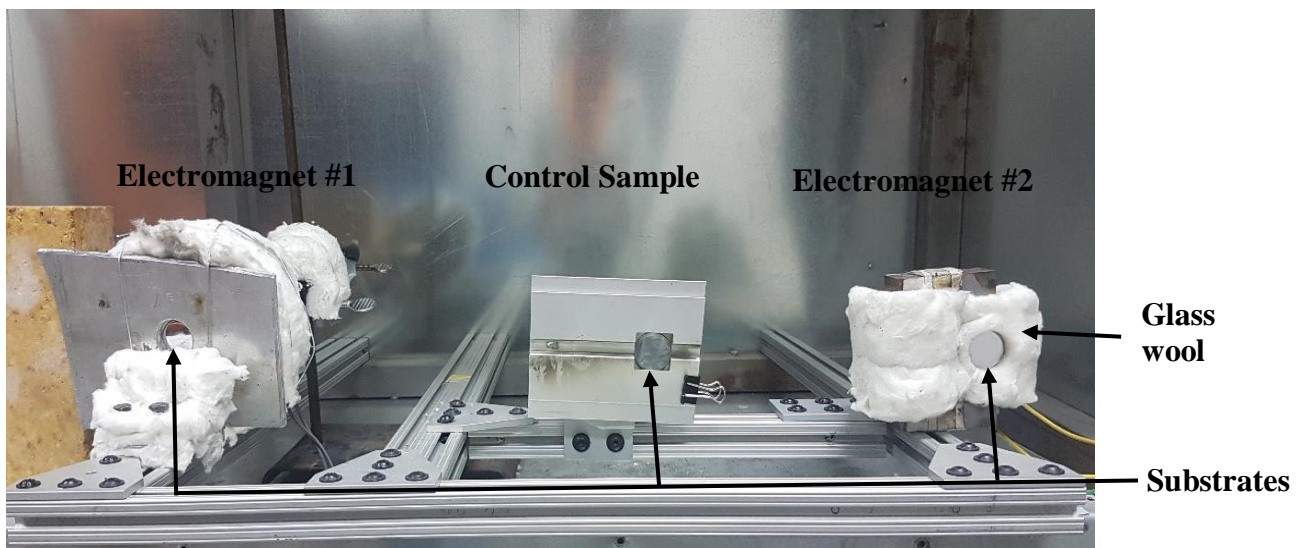


Figure 8. Experimental set-up, front view.

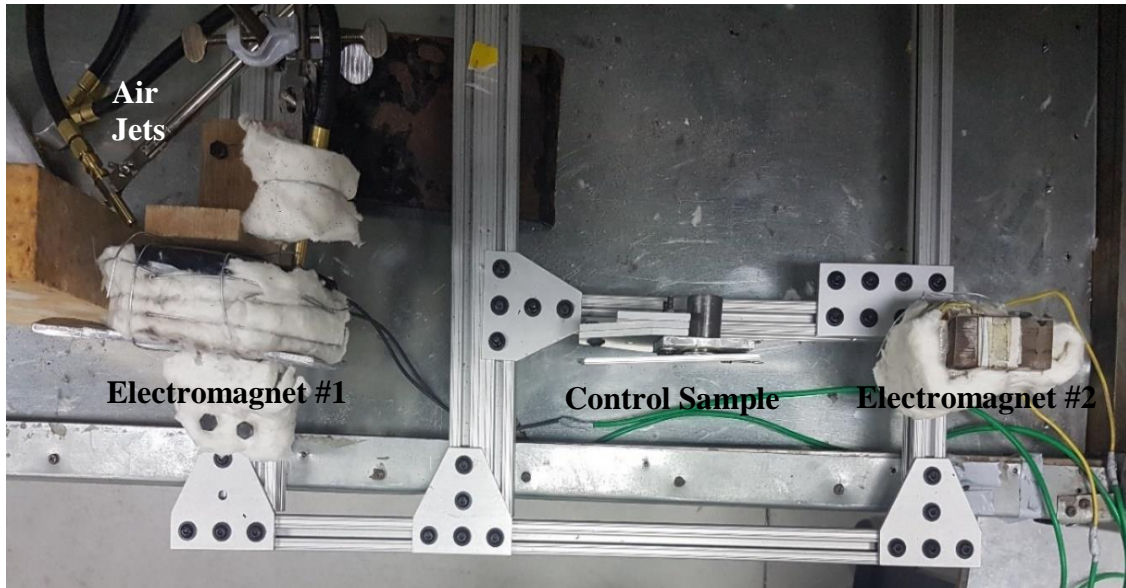


Figure 9. Experiment set-up, top-view. Air jets were used to cool down the coil of electromagnets.

The magnetic field generated by each electromagnet were measured with a gaussmeter (F.W. Bell Model 5080, USA) that uses the hall-effect principle. Electromagnet #1 generates a magnetic field perpendicular to the substrate that varies from 0.15 to 0.35 [T] at the surface. On the other hand, Electromagnet #2 generates a parallel magnetic field that varies from 0.04 – 0.09 [T] at the surface.

Methodology

Three samples with different conditions were sprayed for each material in the form of splats, that is: 1) samples with electromagnetic field parallel to the substrate surface, 2) samples with electromagnetic field perpendicular to substrate surface, and 3) control samples without any electromagnetic influence. Only Ni powder was thermally sprayed in the form of coating, two for each sample conditions. The total samples produced are described in Table 1.

Table 1. Number of samples produced by flame spaying under different conditions of applied magnetic field.

Powder	Type of sample	Parallel Electromagnetic Field	Perpendicular Electromagnetic Field	Referential (without electromagnetic field)
Ni	Splats	1	2	2
	Coating	2	2	2
NiCr	Splats	1	1	1
NiCrBSiFe	Splats	1	1	1

The samples were preheated under similar experimental conditions using the same TS torch; a pyrometer (Fluke 62 MAX+, WA, USA) was used to monitor the preheating temperature of 200°C. The deposition parameters for flame spaying are described in Table 2.

Table 2. Spraying parameters for sample preparation.

Parameter	Magnitude
Air pressure	14.5 psi
Acetylene pressure	13 psi
Acetylene Flow Rate	40 SCFH
Oxygen pressure	30 psi
Oxygen Flow Rate	45 SCFH
Spray distance	150 mm
Spray angle	Normal to surface

To assure that the testing variable is only the change in electromagnetic field, and therefore any noticeable difference can be attributed to it, all spraying parameters were kept constant, and all the substrates were placed in a row in each process run. For instance, Ni powder was deposited in the same trial over three substrates: one with parallel

electromagnetic field, one with perpendicular electromagnetic field, and one without the presence of an electromagnetic field.

Characterization

Splats were first analyzed using an optical microscope (Nikon MA200, MI, USA). Changes in splat morphology were observed, and further analysis was required. Second, an analytical scanning electron microscope SEM (JEOL JSM-IT300LA, Japan) was used to detect specific effects in splat morphology. In addition, powders and as-sprayed top-surfaces of the coatings were also analyzed with the SEM.

The ASTM C633-13 Standard Test Method for Adhesion or Cohesion Strength of Thermal Spray Coatings was chosen for the adhesion/cohesion strength tests due to its low cost and accessibility. An adhesive bonding agent (Master Bond EP15ND-2, NJ, USA) was used to attach the coated substrate with the counterpart substrate. EPN15ND-2 technical data sheet was followed for adhesive application and cure processes. Adhesion tests were performed using a universal testing machine (Tinius Oisen 300 SL, PA, USA) at room temperature. This machine was used to apply a strain rate of 0.015 [mm/s] to each tested sample until rupture occurred. The adhesion/cohesion strength of the thermal sprayed coatings were determined from the tensile load applied right before rupture occurred.

RESULTS AND DISCUSSION

Powders were analyzed with SEM. As illustrated in Fig. 10, Ni-powder is a coarse grade material that exhibits particles with globular morphologies, agglomerated clots, and rough surfaces; the nominal particle size distribution is $-45 +45$ [μm]. NiCr-powder is a fine grade material that exhibits particles with spherical and irregular morphologies, with smoother surfaces than Ni -powder; the nominal particle size distribution is $-63+10$ [μm]. NiCrBSiFe-powder has a nominal particle size of $-140+20$ [μm].

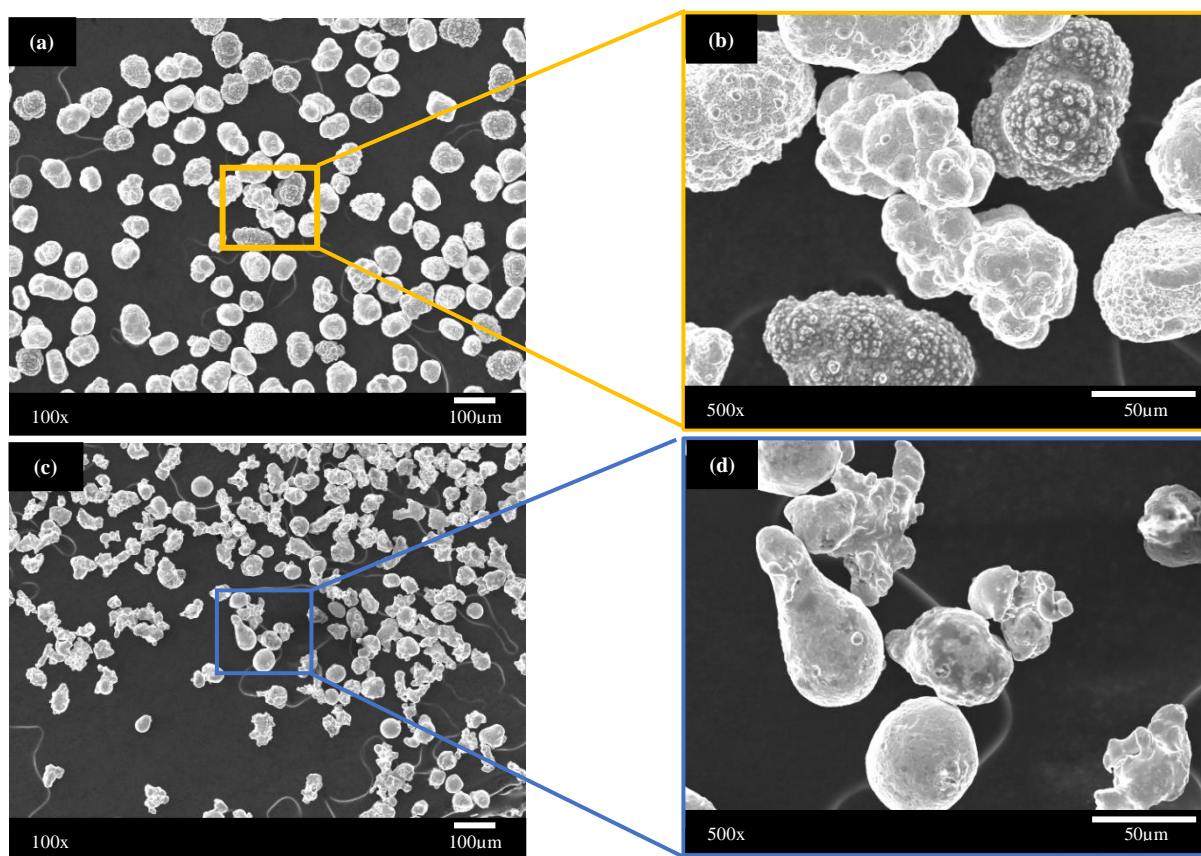


Figure 10. SEM images of powders used for thermal spraying: a) Ni Powder; b) Ni Powder high magnification; c) NiCr Powder; d) NiCr Powder high magnification.

Ni-powder was chosen for thermal spraying under perpendicular electromagnetic field, only. Splats that were applied with this influence showed a different morphology compared with the ones applied without the electromagnetic field, see Fig. 11. A tendency to

form disk-shaped splats were found in the substrate, and a well-shaped nucleus can be identified near their center, Fig. 11c and Fig. 11d.

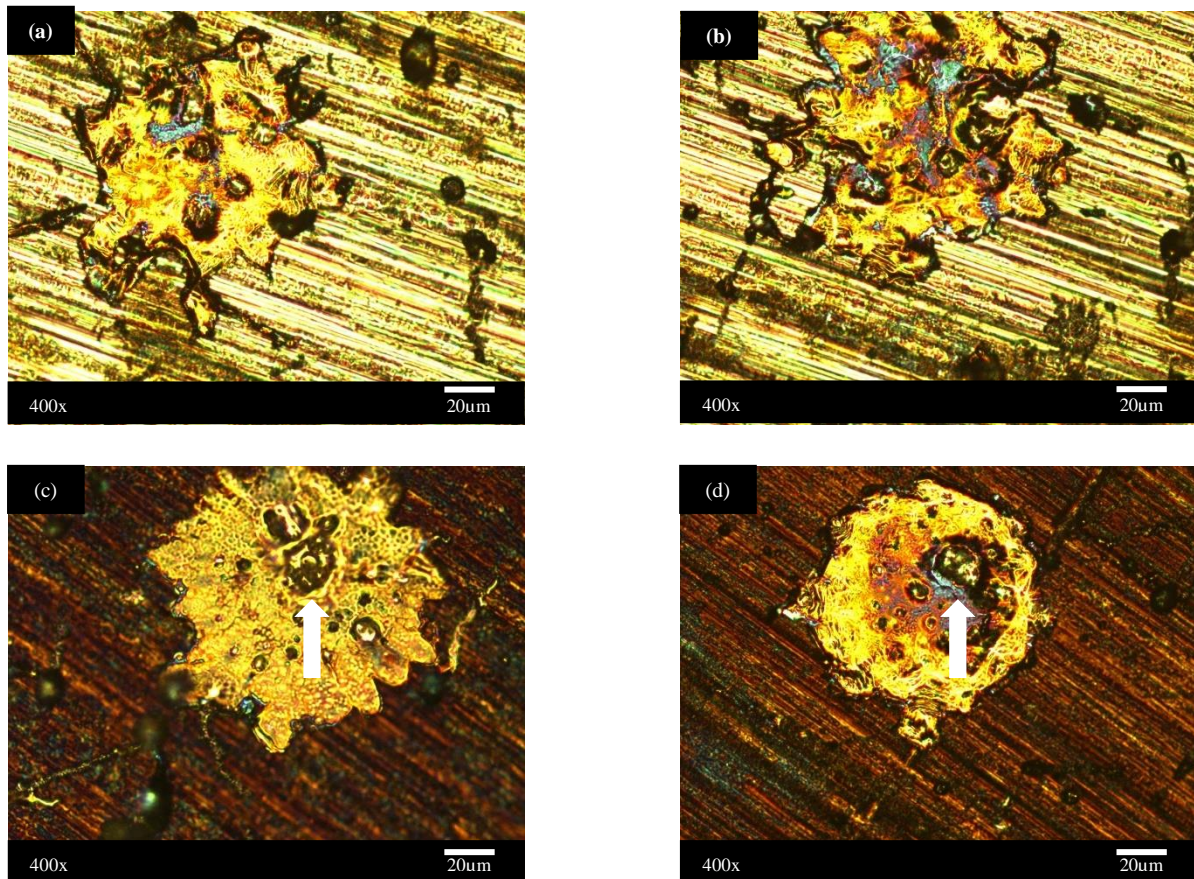


Figure 11. Ni splats by flame spraying: a) and b) Splats formed without electromagnetic influence; c) and d) Splats formed with perpendicular electromagnetic influence. The white arrows point splats nucleus.

It is believed that these nuclei are formed due to the electromagnetic field and Ni-based particles interaction. Ni is a metal that can be polarized under the influence of a magnetic field. Indeed, when the Ni-based particle is travelling towards the substrate, it is magnetically polarized due to the action of the electromagnetic field. Since the field is perpendicular to surface (i.e. same direction of the particle motion before impinging, see Fig. 2) the polarization leads to a magnetic attraction force, due to the positive magnetic field gradient. This attraction force also imposes momentum to the particle that could have some effects, for instance: it could allow a better particle-substrate adhesion, better particle-particle cohesion, or induce to an inelastic collision causing particles to rebound. Right after the

participle impacts the substrate surface, the molten particle flows over the substrate surface. Regarding magnetohydrodynamics principles, the molten participle experiments a Lorentz force acting as a fluid flow suppressor. This influence encapsulates the molten participle leading to the disk-shaped splats showed in Fig. 11c and Fig. 11d.

The optical microscope started the analysis path of splat morphology, however because of its focusing limits further analysis with SEM was needed for all the samples. In Fig. 12a splashed splats were found, while in Fig. 12b a tendency to form disk-shaped splats were found.

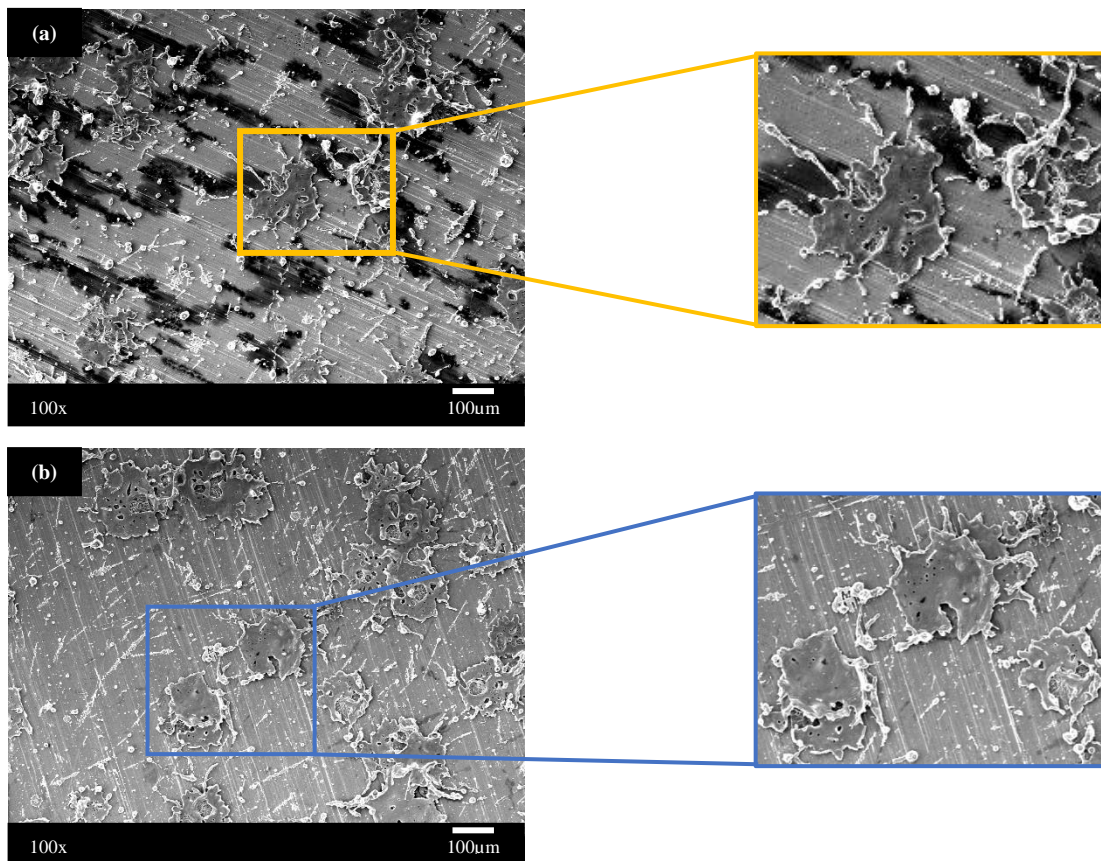


Figure 12. Typical Ni splats by flame spray, using SEM: a) Splats formed without electromagnetic influence; b) Splats formed with perpendicular electromagnetic influence.

A second trial was performed using Ni Powder, this time three samples were sprayed including the sample with parallel electromagnetic influence. As illustrated in Fig. 13a and 13b, typical splashed splats with deep dimple were found in the sample without magnetic

influence. An interesting phenomenon occurs with the sample influenced by perpendicular electromagnetic field; as it can be seen in Fig. 13c and 13d partially molten particles adheres to the substrate. Despite thermal spraying with the same torch stream onto the three samples, neither the control sample nor the parallel influenced showed partially molten particles. This phenomenon suggests that the sample influenced with perpendicular field interact with the molten particles in a way to make them rebound, and just the partially molten (or solid) particles adhere to the surface. Two types of splats were found in the parallel influenced sample, first Fig. 13e shows a splat with a flow tendency in one preferential direction, and second a dramatically broken splat highlighting neither with splashing as Fig. 13a nor branches.

The Hartmann number was calculated only for Ni particles because of the availability of the electric conductivity and dynamic viscosity in academic references. For instance, the electric conductivity of Ni is 14.3×10^6 [Siemens/m] and the dynamic viscosity is 5×10^{-3} [Pa/s]. In a conservative scenario, the magnetic field used in the Eq. 5 of the Hartmann number was selected as the lowest magnetic field measured in the electromagnets; the characteristic length was selected as half the diameter of a 100 [μm] Ni particle. Following Eq. 5, the Hartmann numbers for perpendicular influence and parallel influence are 8.46 and 3.38. Thus, the electromagnetic forces dominate over the viscous forces in the rapid solidification of Ni splats.

NiCr splats were deposited onto the three types of sample, as illustrated in Fig. 14. Since the NiCr particles size is smaller than the Ni particles, a high magnification was needed. These samples contain few residues of particles, finer than splats that are distributed among the substrate. The control sample showed splats with a typical splashed and branched morphology, Fig. 14a and 14b. The sample with perpendicular influence showed a disk-shaped splat formation tendency with a smooth surface, and many of the remains particles

agglomerated around the splat, Fig. 14c and 14d. Finally, the sample influenced with parallel field showed oval- shaped splats with a rough surface; Fig. 14e shows a splat formed from a molten particle in contrast to Fig 14f that shows a solid particle. None of the electromagnetic influenced samples showed splashed splat nor splats with prominent branches.

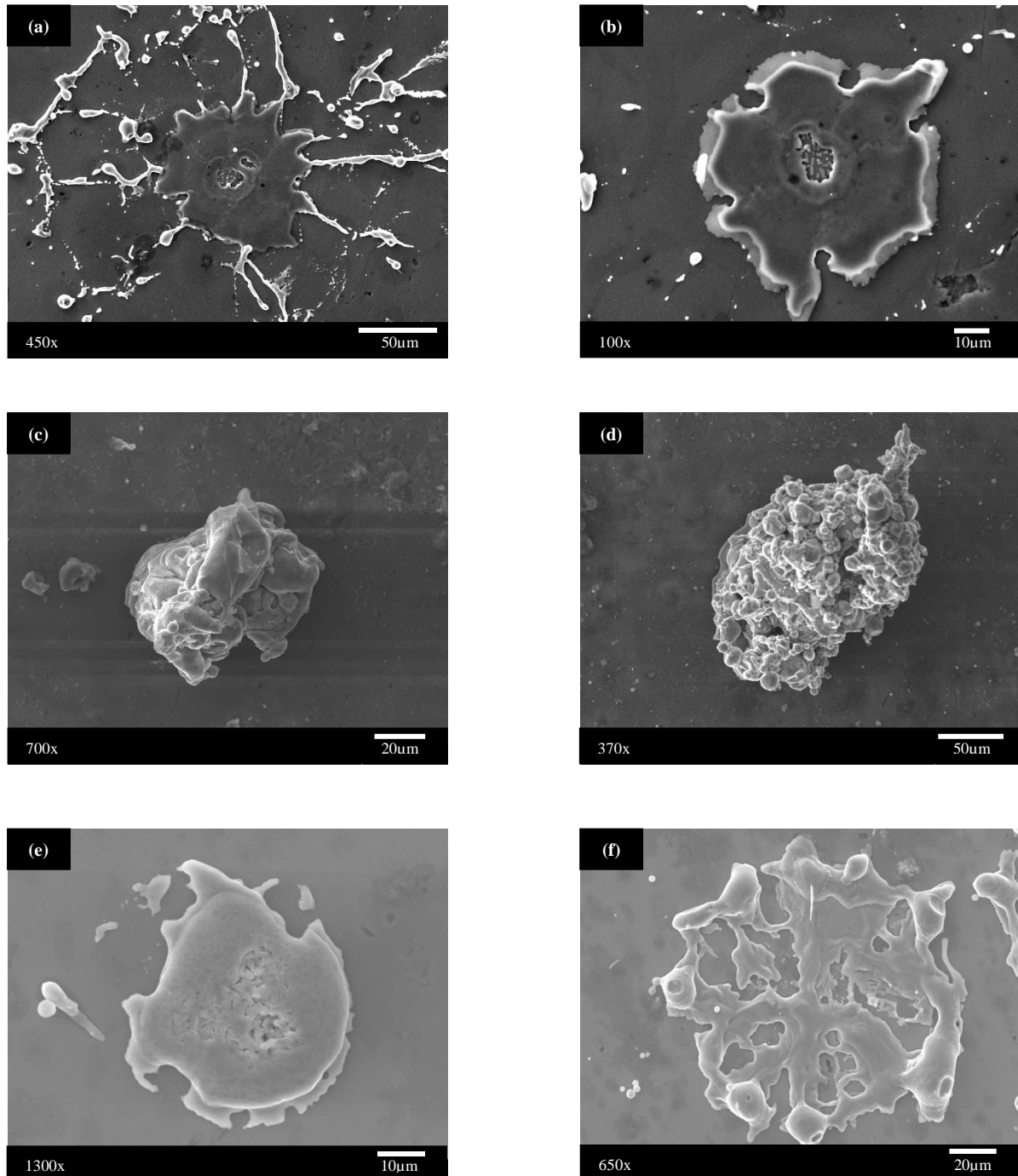


Figure 13. Second trial, typical Ni splats by flame spray: a) and b) Splats formed without electromagnetic influence; c) and d) Splats formed with perpendicular electromagnetic influence; e) and f) Splats formed with parallel electromagnetic influence.

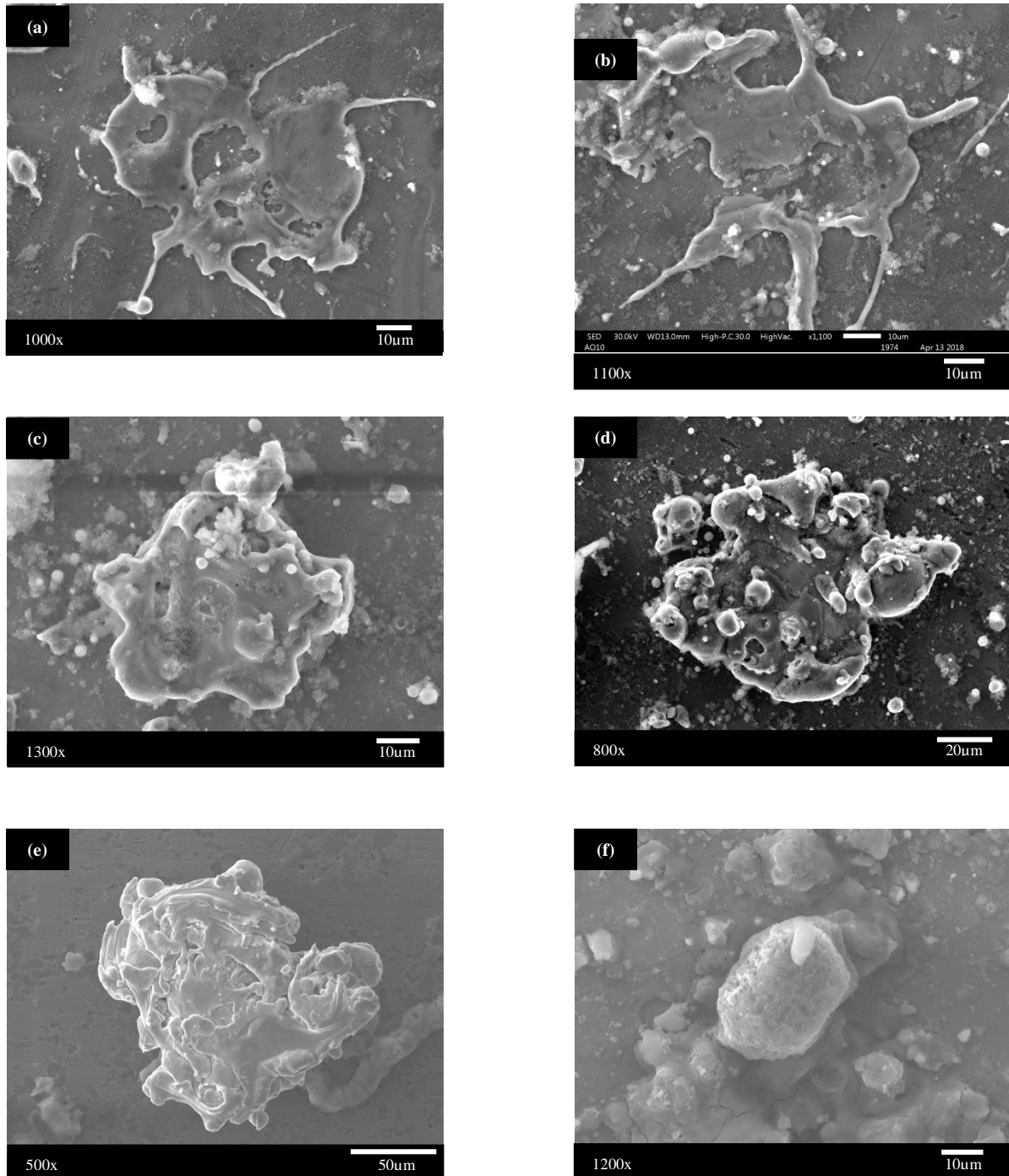


Figure 14. Typical NiCr splats by flame spray: a) and b) Splats formed without electromagnetic influence; c) and d) Splats formed with perpendicular electromagnetic influence; e) and f) Splats formed with parallel electromagnetic influence.

The last splat deposition experiment was performed with the NiCrBSiFe Powder. As illustrated in Fig. 15a and 15b., splashed splats were formed. In addition, rests of particles adhered to the substrate and also to the splats, suggesting that splashing was prominent in this sample. The sample with perpendicular influence showed an interesting phenomenon. Splats

did not adhere to the substrate, despite the torch beam was pointed four times onto the sample. When analyzing this sample just a very few particles adhered to the substrate, a typical splat for this case is shown in Fig. 15c. At a first sight, it was hypothesized that the particles were repelled by the electromagnetic field considering particles with magnetic polarization. However, further analysis in the substrate showed that the molten particles impinged the surface and rebounded. Multiple marks caused by molten particles were visualized in this sample. Fig. 15d illustrates a typical mark where a heat affected zone can be clearly seen. Finally, influenced sample with parallel electromagnetic field showed a preferential flow of the molten particles. The splat shapes cannot be clearly determined contrary to the splashed splats or disk-shaped splats on other samples, Fig. 15e. Nevertheless, the splat appearance shown on Fig. 15f suggest a fluid flow in a preferential direction forming *paths*. Fluid flow paths are illustrated on Fig. 16.

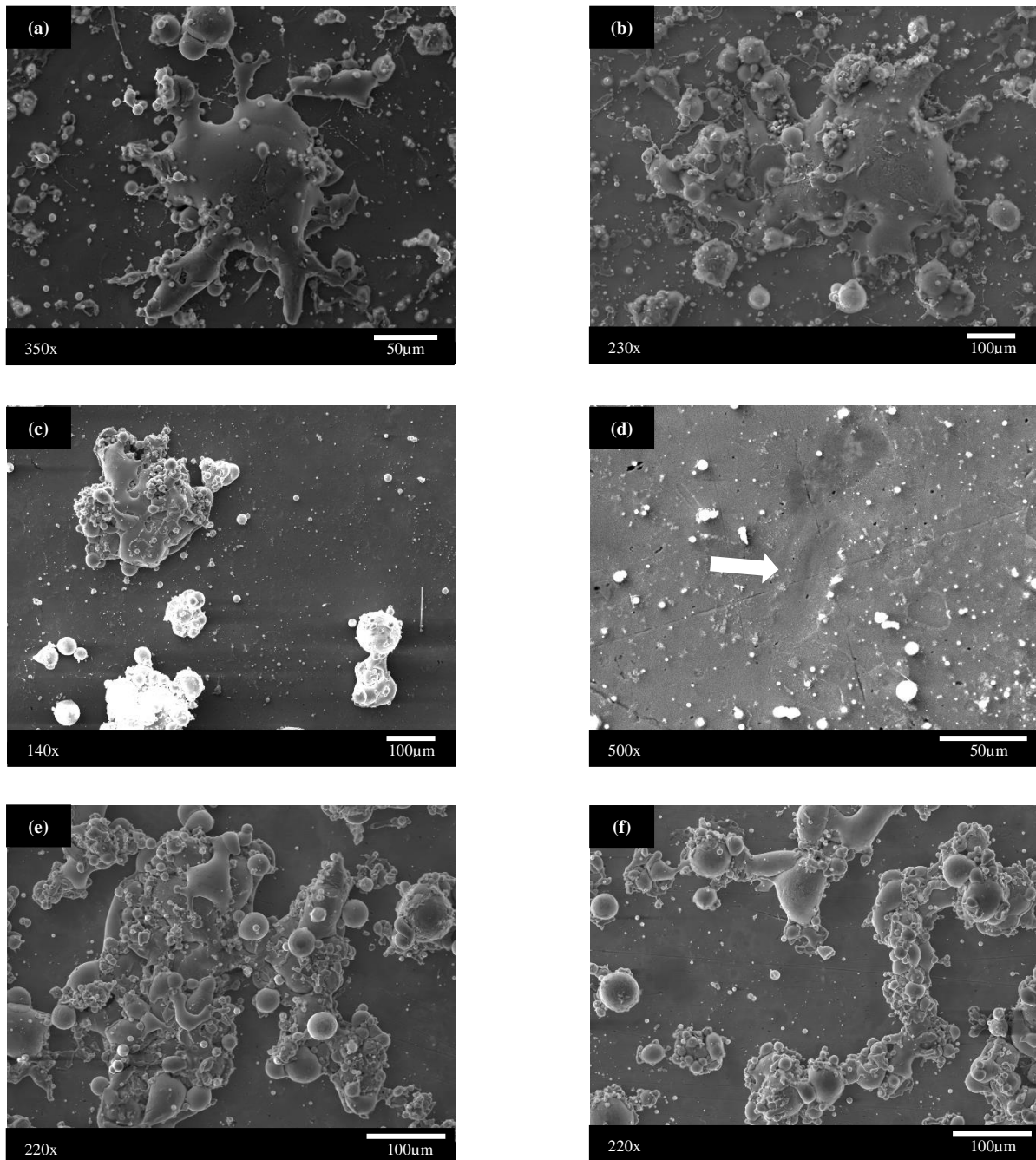


Figure 15. Typical NiCrBSiFe splats by flame spray: a) and b) Splats formed without electromagnetic influence; c) Splats formed with perpendicular electromagnetic influence; d) Impinging marks over all the surface, white arrow points the heat affected zone. e) and f) Splats formed with parallel electromagnetic field influence.

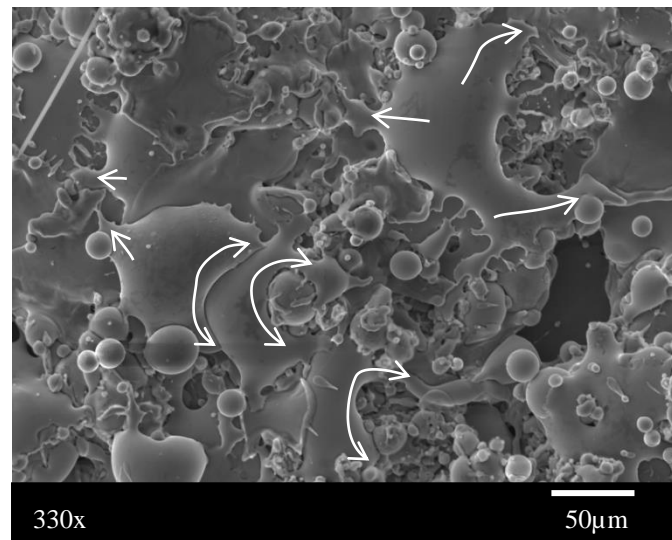


Figure 16. Fluid flow paths of NiCrBSiFe splats with parallel electromagnetic field influence.

A final SEM analysis was conducted on coating surfaces deposited on the control and perpendicular influenced sample. Fig. 17a shows the surface of a Ni coating deposited onto the control sample; splashing and a rough surface can be seen. On the other hand, on the Ni coating deposited onto the perpendicularly influenced sample, less splashing and a smoother surface can be observed. Less splashing could lead to a better adhesion/cohesion strength because of an improvement in splats interface contact, i.e. splats allocate better on top of another one, and fill more surface without any splashing obstacles.

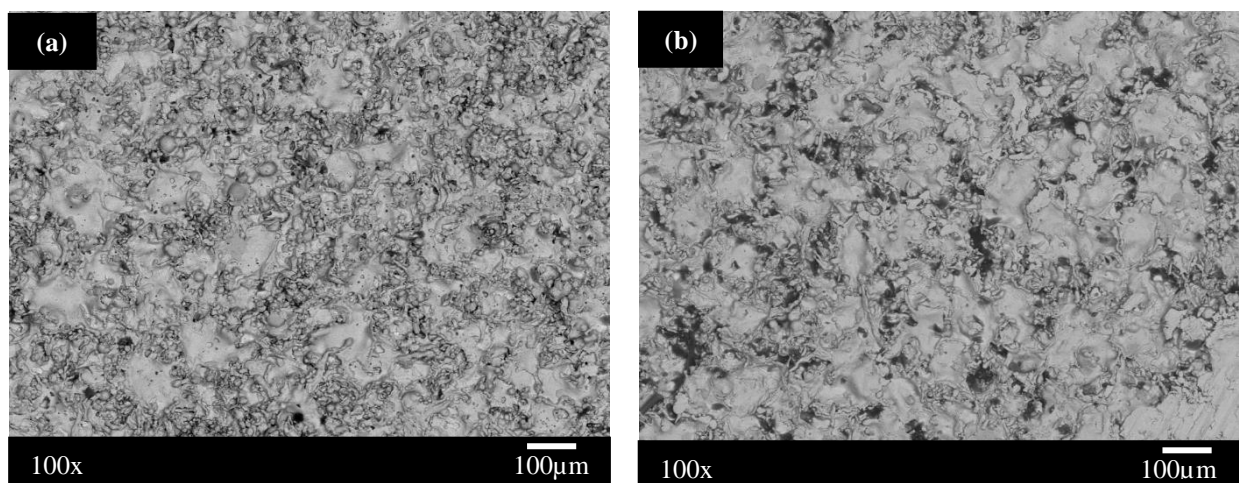


Figure 17. Ni coating by flame spray: a) Coating deposited without electromagnetic influence; b) Coating deposited with perpendicular electromagnetic influence.

Finally, Ni coatings with a thickness of 0.5 to 2 [mm] were obtained with and without applied electromagnetic field during deposition. The adhesion was measured under the ASTM C 633 Standard Test Method for Adhesion or Cohesion Strength of Thermal Spray Coatings, and the results are shown in Fig. 18. As contrary as expected, the adhesion of coatings under the effects of a d.c. electromagnetic field was weakened by 30%.

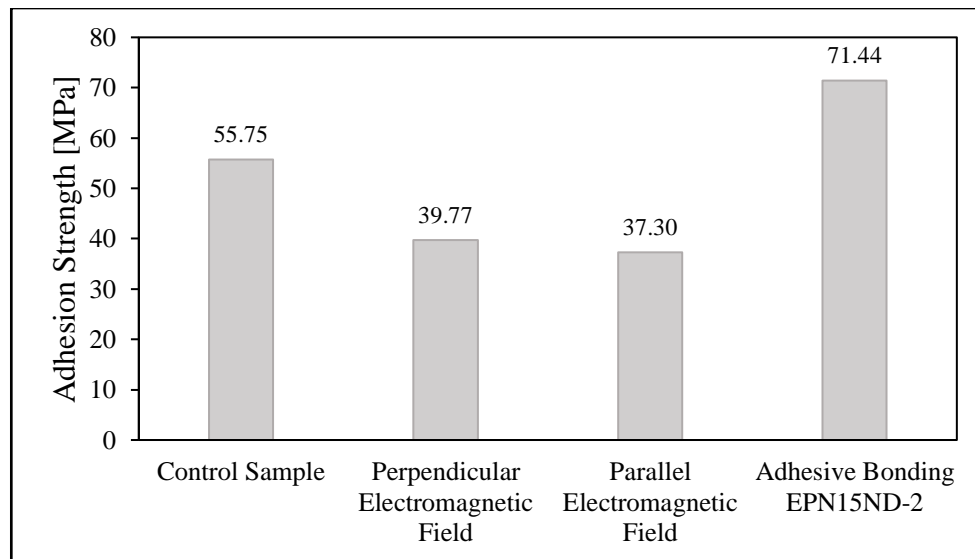


Figure 18. Adhesion strength of coatings with and without electromagnetic influence during deposition. The adhesion strength of the adhesive bonding EPN15ND-2 is also shown.

The adhesion tests indicate that electromagnetic field weaken coating adhesion no matter the direction of the field. The adhesion was not evaluated in the splat morphology analysis; however, the adhesion test results closed this gap.

Considering that for a perpendicular electromagnetic field, splashing was reduced but a rebound effect was observed. Since the torch beam carries millions of particles, there is a high probability that the rebound particles collide with another *fresh* particle. Different effects could be caused by this collision, for instance it could reduce not only the rebound particle momentum but also the *fresh* particle momentum; the rebound particle returns to a partially molten state and could break the *fresh* particle; or the collision could change the

velocity direction of each particle. No matter which effect happened, a lower quality adhesion coating is expected.

Secondly, for parallel electromagnetic field some fluid flow direction preferences were observed from splats morphology, and also splashing was reduced. However, this type of electromagnetic field can shape the splat accordingly to the direction of the field, the characteristic, and always wanted, disk shape is distorted. From Fig. 15e and 15f it can be inferred that splats will be aligned in a preferential direction creating paths where *fresh* splats will be allocated, and indeed distorted again. This distortion effect could be the cause for weaken the coating adhesion/cohesion.

CONCLUSIONS

Electromagnetic field was introduced as a new control variable in thermal spray, specifically in flame spray. Simulations with the software FEMM were performed in order to design electromagnets capable to generate the desired electromagnetic field. Ni, NiCr, and NiCrBSiFe splats were deposited onto AISI 1018 steel substrates under the influence of parallel and perpendicular electromagnetic fields. Splat morphologies were analyzed and compared to the control sample. In addition, the adhesion of Ni coatings influenced by electromagnetic fields were tested under the ASME C633-13 standard.

The application of an electromagnetic field, regardless of perpendicular or parallel direction, during splat formation has shown to have an influence in splats morphology, thus in adhesion strength. The application of direct current electromagnetic field reduces significantly splat splashing and increases the probability to produce a disk-shaped morphology. Specifically, a d.c. electromagnetic field from 150 to 350 [mT] perpendicular to the substrate surface, reduced the spreading and splashing of the splat leading to disk-shaped splats; impinging marks were found in the substrate concluding that particles had rebounded; and the adhesion strength was weakened by 30%. A d.c. electromagnetic field from 40 to 90 [mT] parallel to the substrate surface, reduced splat splashing however splats suffer spreading in a preferential direction perpendicular to the electromagnetic field; and also, the adhesion strength was weakened by 30%.

Despite the fact the adhesion strength was reduced with d.c. electromagnetic fields, further studies are needed to fully understand the effects of this influence. It is suggested that future analysis should: aim to eliminate the rebound effect varying the perpendicular electromagnetic field magnitude, absolute control of the shape function caused by parallel

electromagnetic fields, AC. Fields, and test this influence of particle state produce for instance by other thermal spray processes such as HVOF or Plasma Spray.

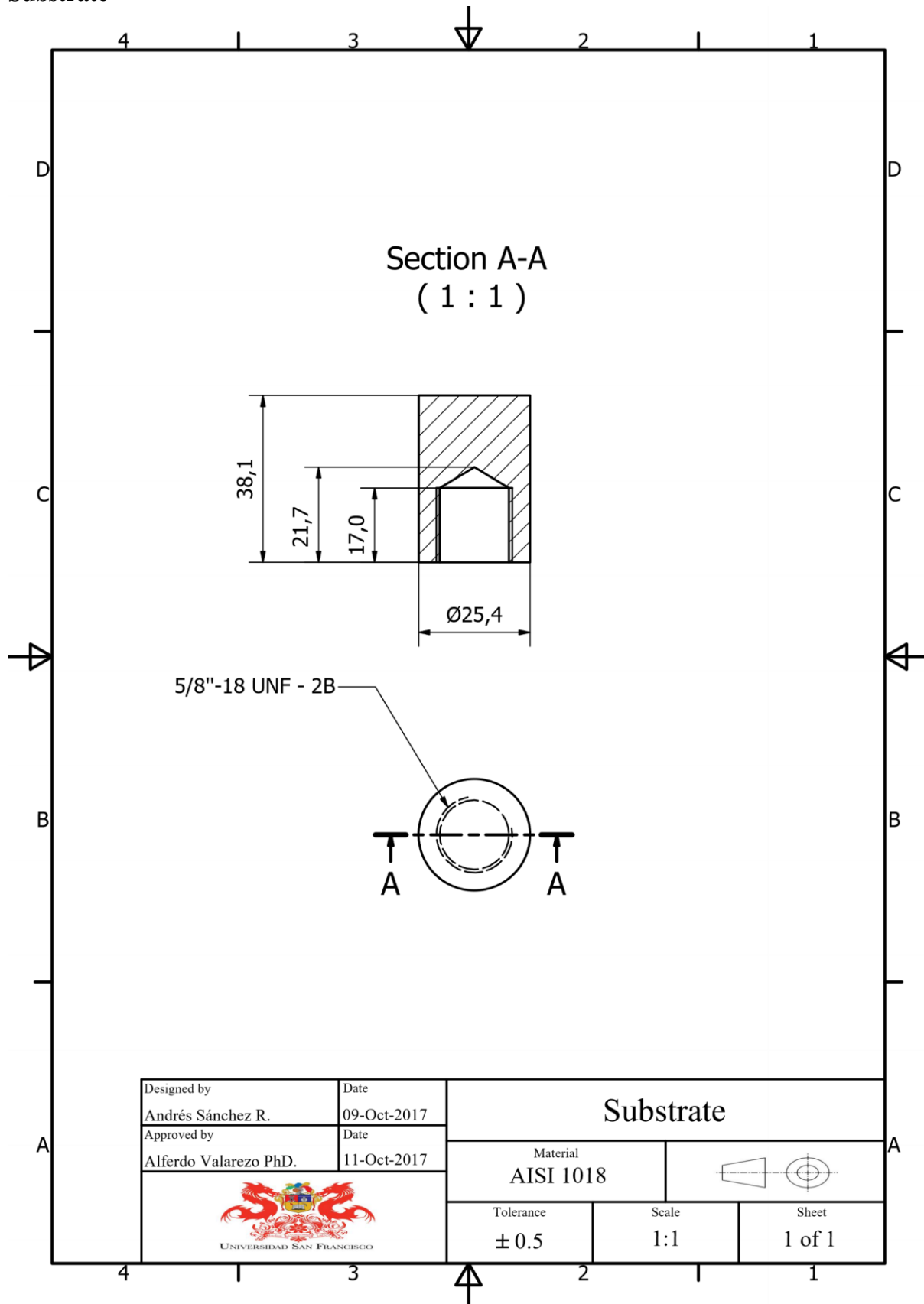
Once the physical principles of these effects are totally understood, a new control variable process can be introduced helping to reduce the gap between first principles, and the thermal spray industry needs.

REFERENCES

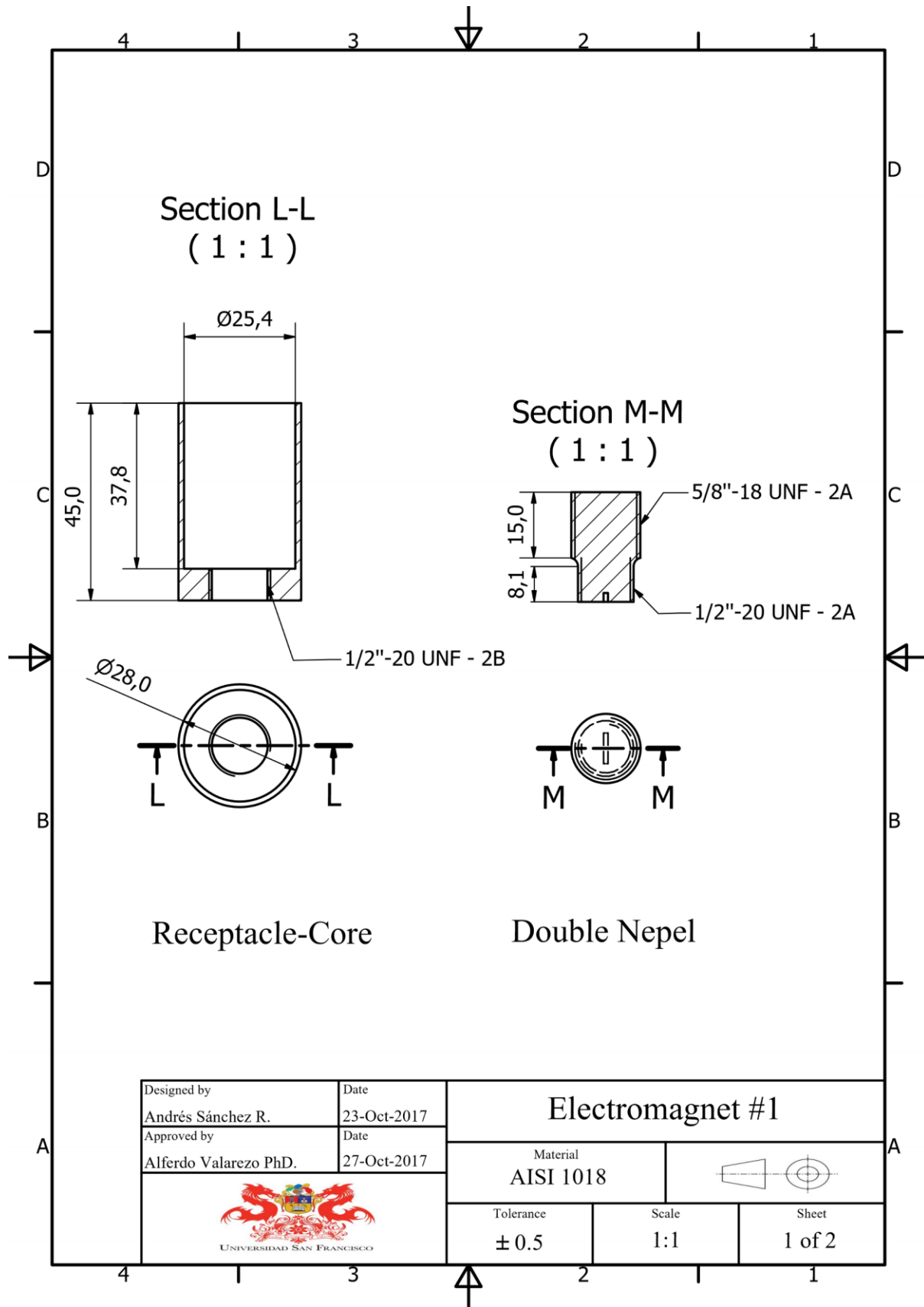
- Asai, S. (2006). *Electromagnetic Processing of Materials* (Vol. 5). Dordrecht: Springer.
- Chandra, S., & Fauchais, P. (2009). Formation of solid splats during thermal spray deposition. *Journal of Thermal Spray Technology*, 18(2), 148–180. <https://doi.org/10.1007/s11666-009-9294-5>
- Fauchais, P., Fukumoto, M., Vardelle, A., & Vardelle, M. (2004). Knowledge Concerning Splat Formation: An Invited Review. *Journal of Thermal Spray Technology*, 13(3), 337–360. <https://doi.org/10.1361/10599630419670>
- Fauchais, P., Vardelle, A., & Dussoubs, B. (2001). Quo vadis thermal spraying? *Journal of Thermal Spray Technology*, 10(1), 44–66. <https://doi.org/10.1361/105996301770349510>
- Li, B. (1998). Solidification Processing of Materials in Magnetic Fields. *Journal of The Minerals, Metals & Materials Society*, 50(2). <http://www.tms.org/pubs/journals/JOM/9802/Li/Li-9802.html#Li>
- Recalde, O., Castro, W., Bejarano, M. L., Vargas, M., & Valarezo, A. (2017). Effect of Electromagnetic Field during Solidification of Ni-Based Alloyed Splats. In *International Thermal Spray Conference & Exposition (ITSC 2017)* (pp. 577–581). Dusseldorf: Curran Associates, Inc.
- Sampath, S., & Jiang, X. (2001). Splat formation and microstructure development during plasma spraying: deposition temperature effects. *Materials Science and Engineering: A*, 304–306(1–2), 144–150. [https://doi.org/10.1016/S0921-5093\(00\)01464-7](https://doi.org/10.1016/S0921-5093(00)01464-7)
- Tharajak, J., Palathai, T., & Sombatsompop, N. (2017). The effects of magnetic field-enhanced thermal spraying on the friction and wear characteristics of poly(ether-ether-ketone) coatings. *Wear*, 372–373, 68–75. <https://doi.org/10.1016/j.wear.2016.11.021>
- Yang, K., Liu, M., Zhou, K., & Deng, C. (2013). Recent Developments in the Research of Splat Formation Process in Thermal Spraying. *Journal of Materials*, 2013, 1–14. <https://doi.org/10.1155/2013/260758>

APPENDIX A: DETAILED DRAWINGS

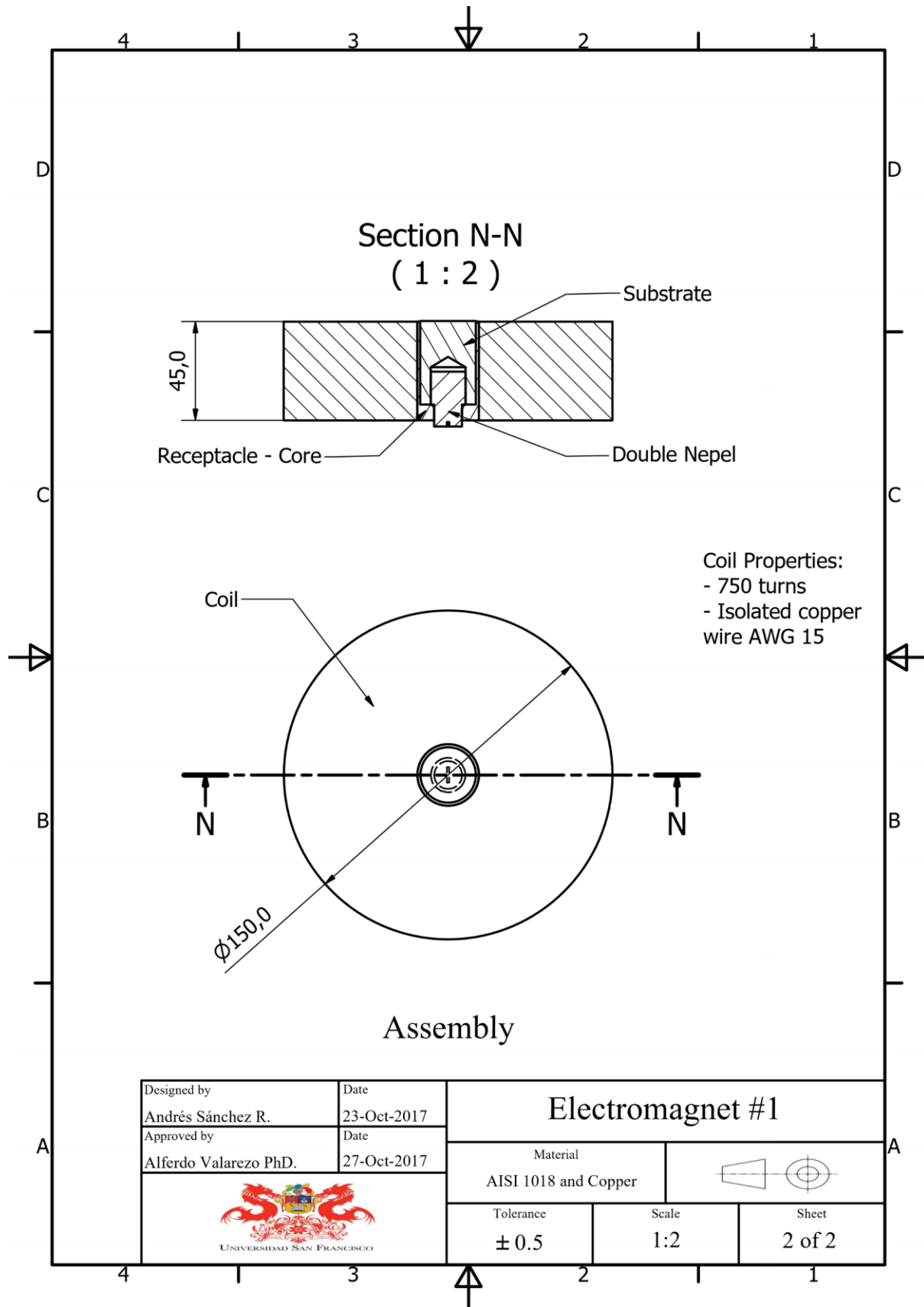
Substrate



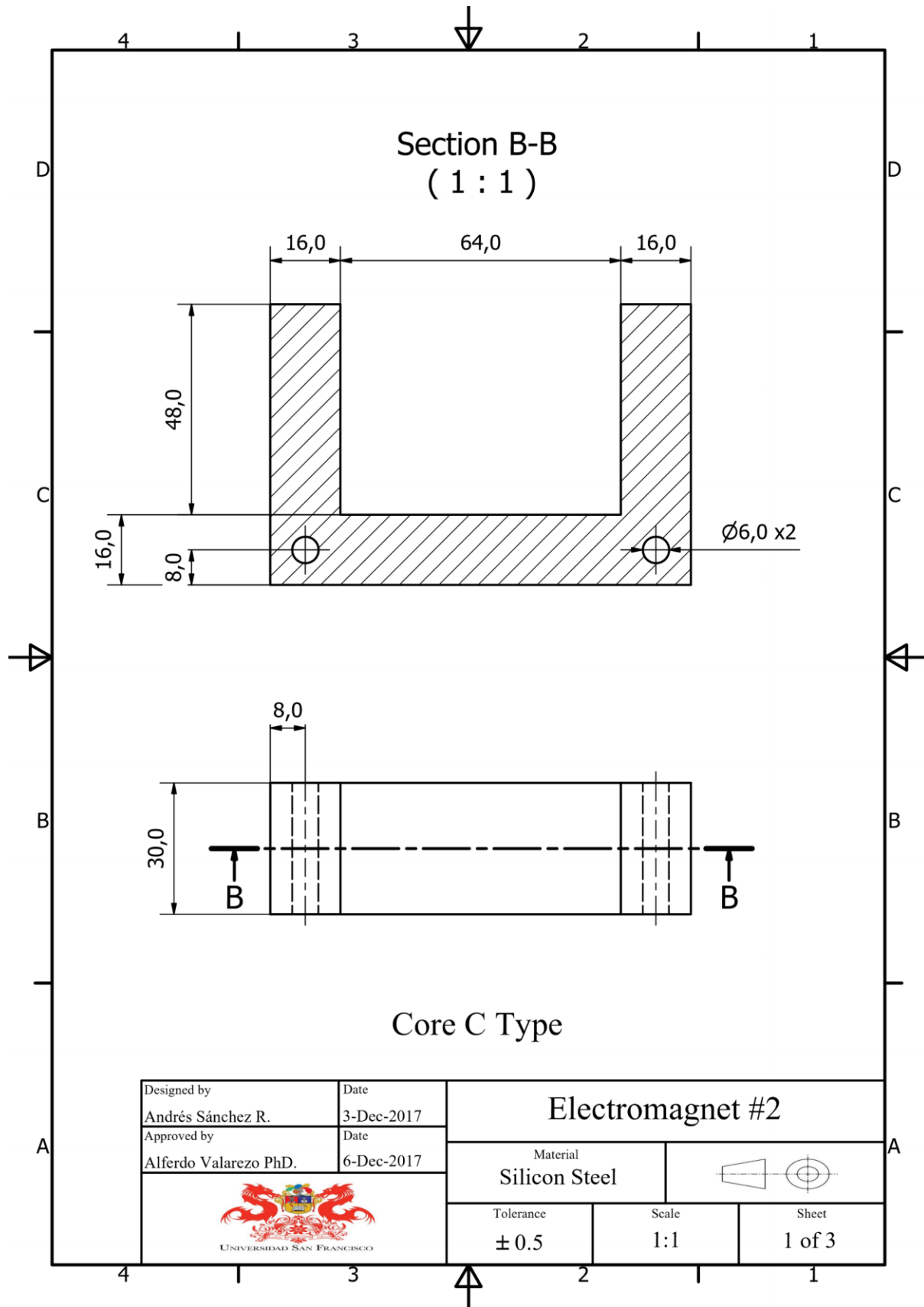
Electromagnet #1: Receptacle – Core



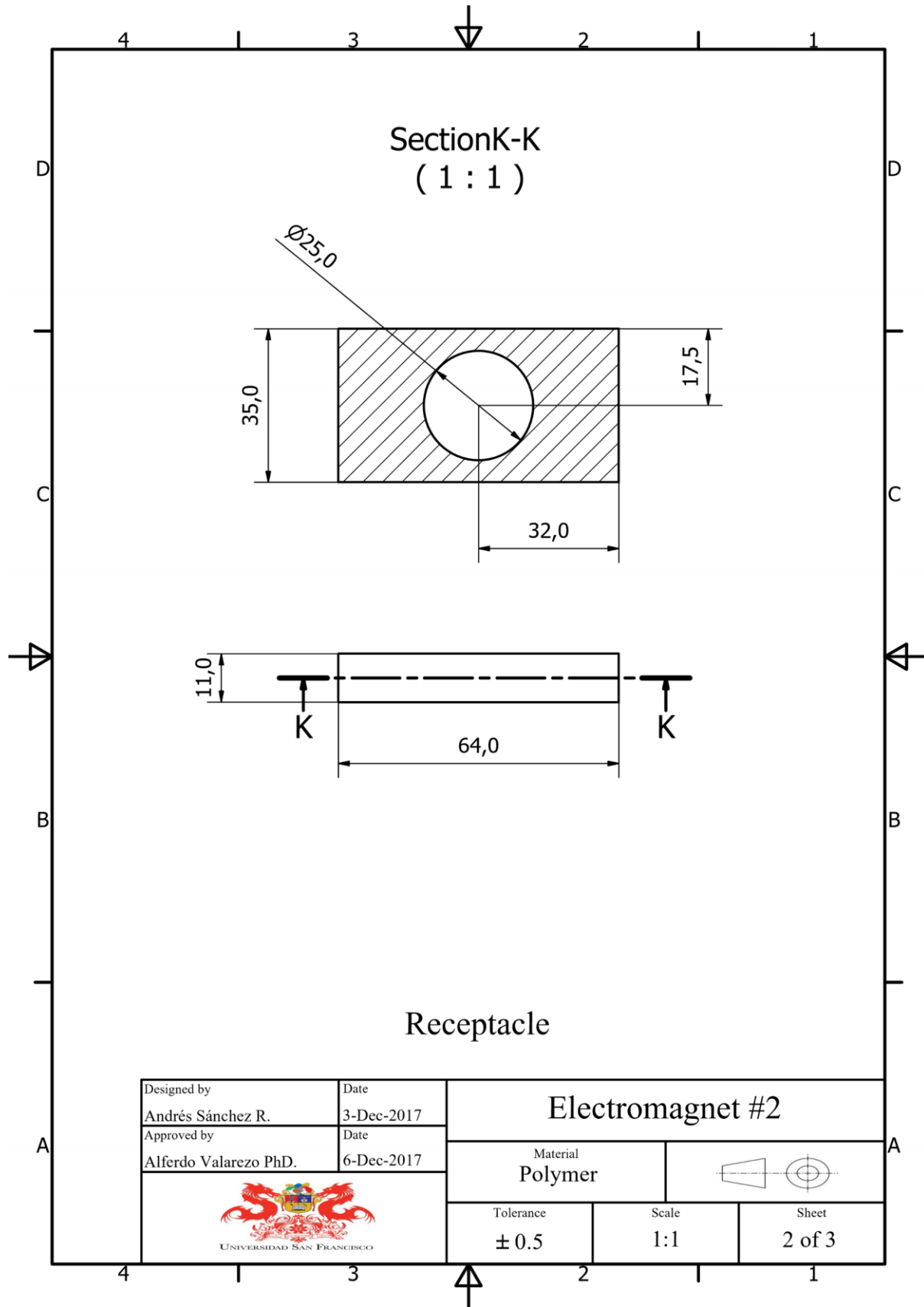
Electromagnet #1: Assembly



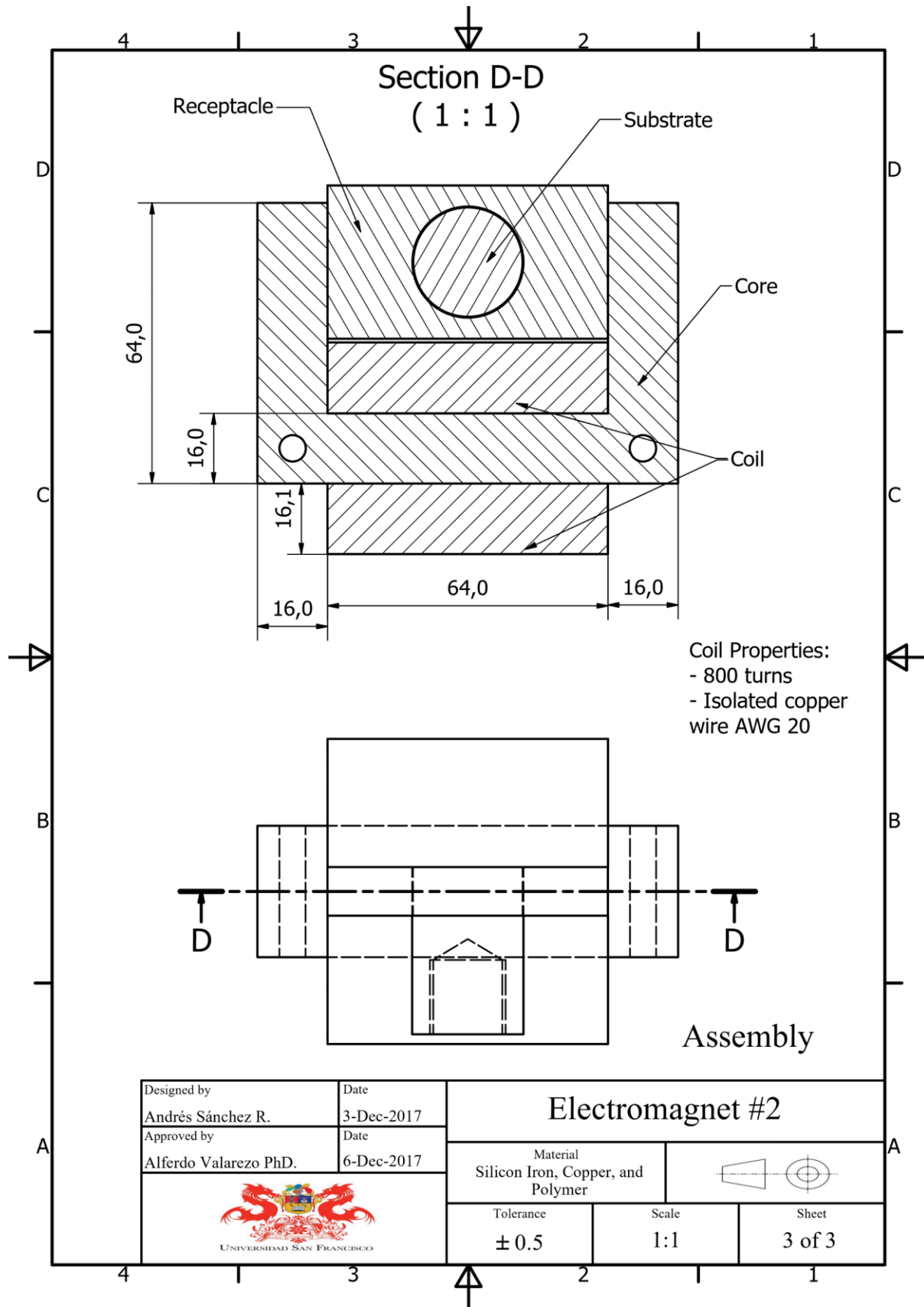
Electromagnet #2: Core



Electromagnet #2: Receptacle

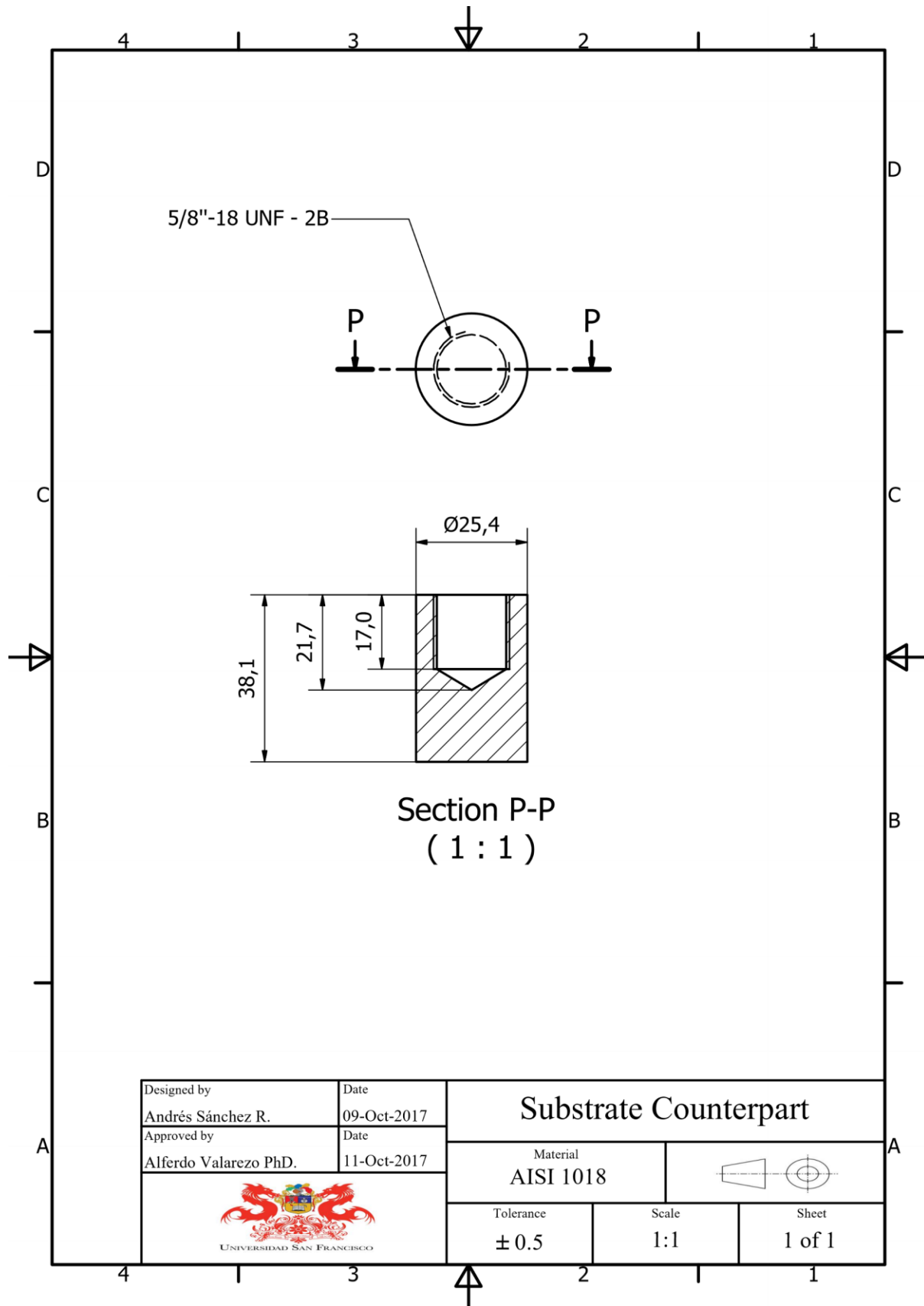


Electromagnet #2: Assembly

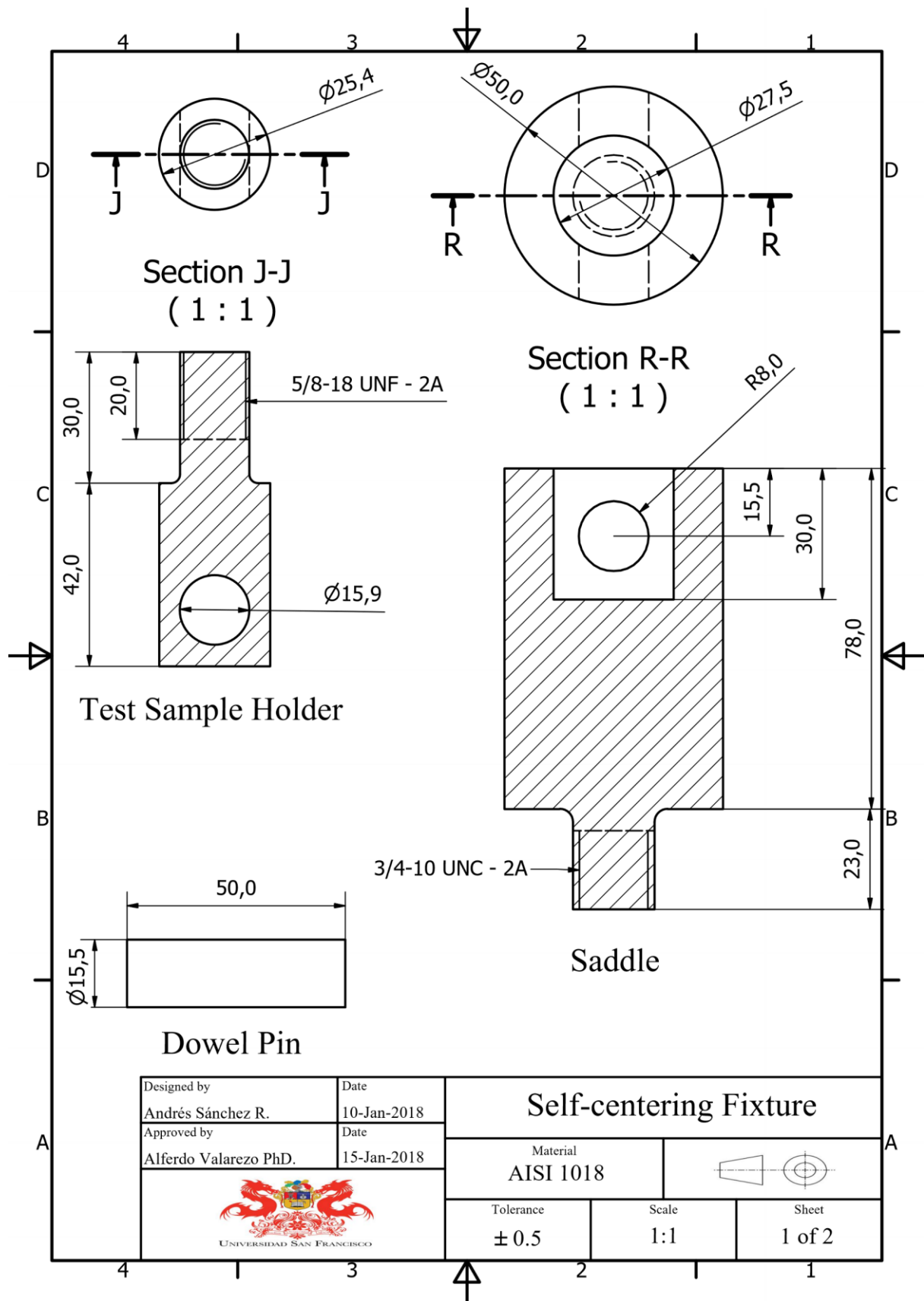


Designed by Andrés Sánchez R.	Date 3-Dec-2017	Electromagnet #2		
Approved by Alferdo Valarezo PhD.	Date 6-Dec-2017			
 UNIVERSIDAD SAN FRANCISCO		Tolerance ± 0.5	Scale 1:1	Sheet 3 of 3

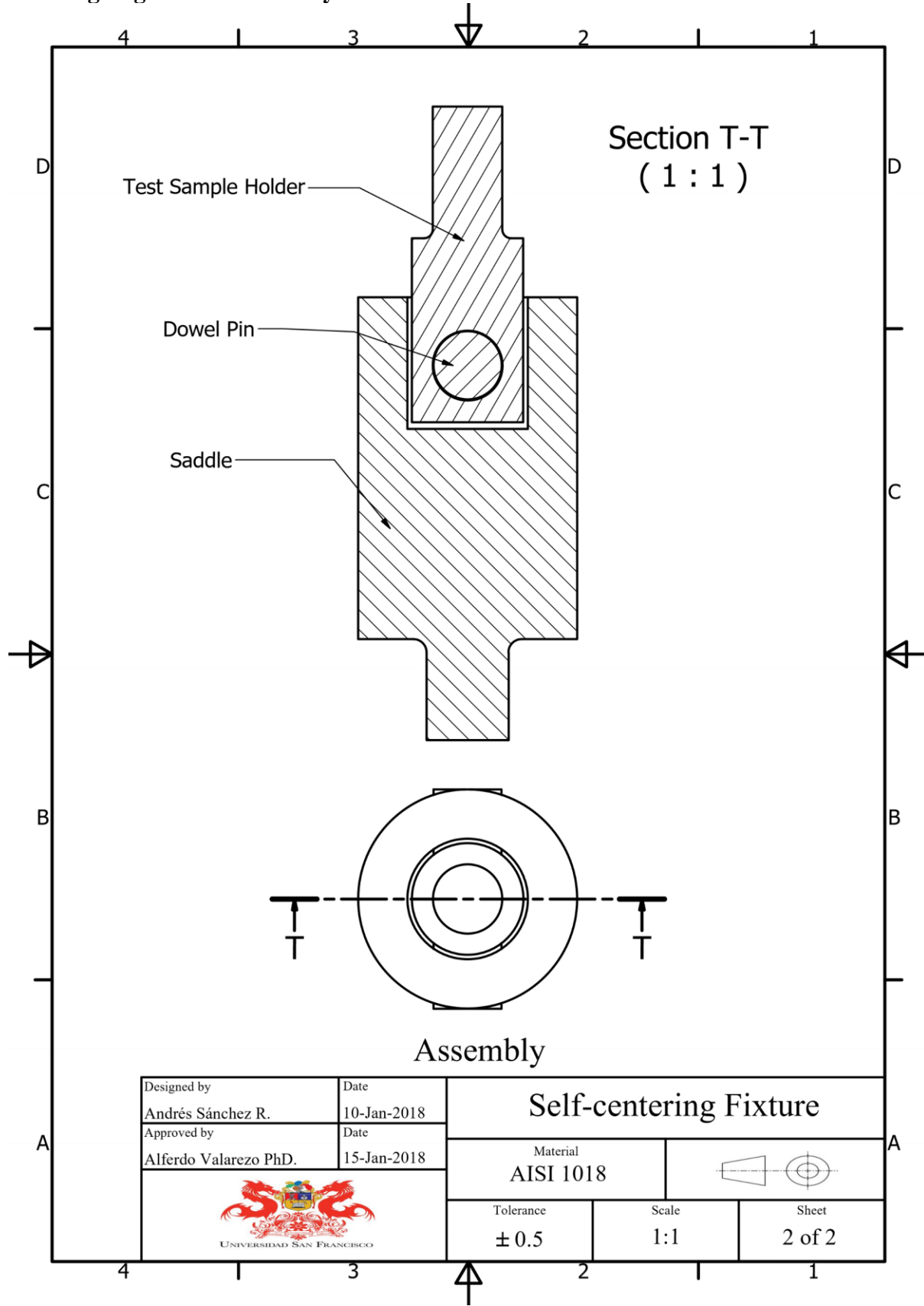
Substrate counterpart



Self-Aligning Device: Parts



Self-Aligning Device: Assembly



Counterpart holder

